Contents of TESLA Report 99-18
Contributions to the 1999 Cryogenic Engineering Conference, Montréal, Canada, July 12-16, 1999

Presented at: ***1999 Cryogenic Engineering Conference***, Montréal, Canada, July12-16, 1999

FRICTION MEASUREMENTS FOR SC CAVITY SLIDING FIXTURES IN LONG CRYOSTATS

D. Barni, M. Castelnuovo, M. Fusetti, C. Pagani and G. Varisco,

INFN Milano-LASA, Via Fratelli Cervi 201, I-20090 Segrate (MI), Italy,

ABSTRACT

Filling factor and static cryogenic losses considerations suggest the use of long multi-cavity cryomodules for high energy superconducting linacs. In the case of TTF/TESLA a further gain has been obtained including the Helium Gas Return Pipe (HeGRP) in the cryostat vacuum vessel and using it as the reference supporting beam for the active elements. One limit of this solution has been the need of developing expensive flexible couplers to feed RF power in the cavities. For cost and reliability considerations in view of TESLA, a new spring loaded sliding fixture, to connect the cavities to the HeGRP, has been developed and qualified at the different operating conditions, from room to cryogenic temperature. Static and quasi-static friction has been measured in a dedicated apparatus for different material coupling and surface finishing. The icing effect in case of a vacuum break has also been studied. The results of this analysis are presented in this paper.

INTRODUCTION

The third cryomodule generation[1] designed for the TESLA Test Facility (TTF)[2] Super Conducting accelerator opens the possibility to use semi-rigid power coupler and superstructures[3]. This result has been obtained by designing a new fixture scheme that decouples the longitudinal position of the cavity string from the structural supporting beam, that is the Helium Gas Return Pipe (HeGRP). During the cooldown, the thermal contractions of the cavity string and of the HeGRP are independent, but the cavity alignment guaranteed by the HeGRP is preserved. Each cavity is now connected to the HeGRP by four low friction sliding fixtures. The qualification tests of this new fixture design are presented in this paper.

SLIDING SUPPORT

As in the previous generation cryostats, in the present design the SC cavities and the quadrupole package are anchored, through the Helium vessels, to the HeGRP which acts as a structural beam for the cold mass and preserves its alignment from room temperature to cryogenic operation.

To appear on: *Advances in Cryogenic Engineering*, Vol. 45
Plenum Press, New York

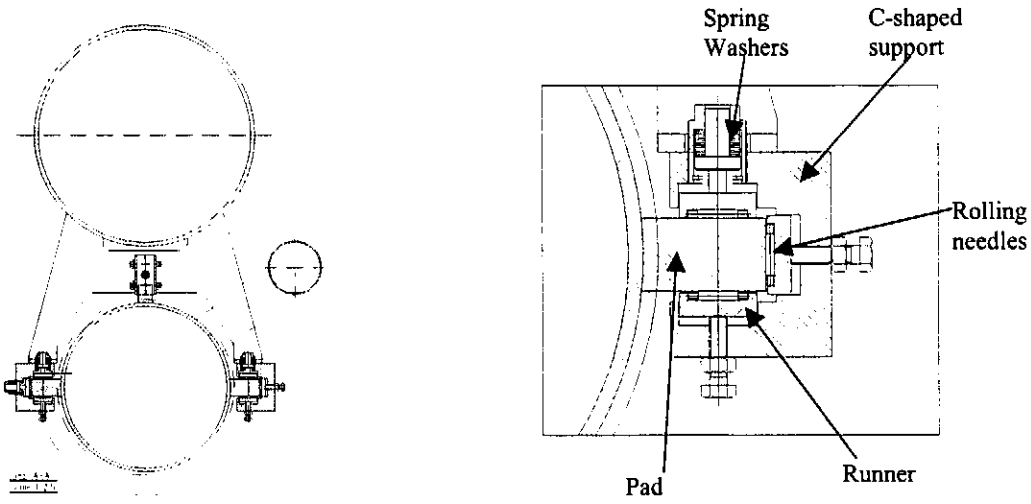

Figure 1. The cavity support scheme. Each cavity is attached to the HeGRP by means of four fixtures. Each fixture includes rollers, runners and reference screws to define the vertical and lateral position. Spring washers are used to give e constant 80 kg_f load. Rolling needles keep the cavity longitudinal position free.

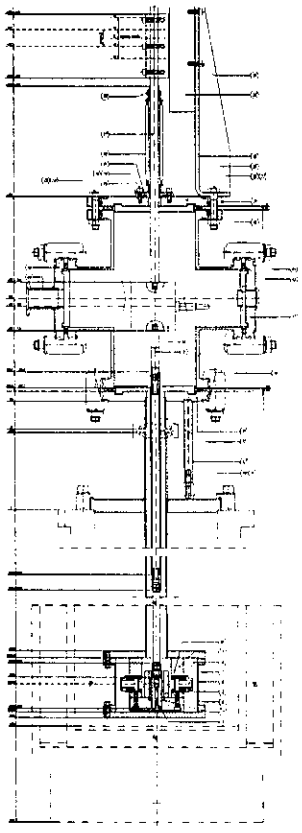

Figure 2. Schematic drawing of the system developed for the sliding fixture measurements.

In the third generation of TTF Cryomodules, new fixture design has been developed in order to adjust and keep fixed the transverse position of the active elements, while leaving the cavity longitudinal position independent from the HeGRP displacements due to the thermal contraction/elongation during cooldown/warmup cycles. This freedom is obtained through a set of low friction rolling needles. The drawing of a cavity anchored by the sliding fixtures is presented in Fig. 1. Each cavity is connected to the HeGRP with four sliding fixtures, each clamping a titanium pad welded on the cavity helium vessel. Each pad fixture consists of a C-shaped stainless steel element that defines the transverse position (with respect to the beam axis) through the sequence of rolling needles, runners and reference screws. In each direction one screw is used for adjustment, while the other is transferring a 80 kg_f force via spring washers. But for the low friction, the longitudinal displacement is independent from that of the HeGRP. The cavity longitudinal position, that could be determined by the use of a rigid coupler solution, is presently fixed via a connection to an independent Invar rod that runs over the cavities and has a fix point at the cryomodule center. This produces a total longitudinal motion of less than 3 mm, which should be compatible with a semi-rigid coupler design.

MEASUREMENT APPARATUS

To qualify the new fixtures a moke-up has been built and a measuring apparatus has been set up. The scheme of the system is shown in Fig. 2. The sliding fixture prototype is

assembled in a vacuum chamber that is part of a properly designed insert for a test cryostat. A motorized computer-controlled linear actuator moves the sliding element with a bellow and a "load cell". The system is designed to test the fixture either under vacuum or at atmospheric pressure. The test temperature, measured by an adequate thermometer system, can range from room temperature to that of liquid Helium. Measurements at 2 K can be taken pumping on the He bath.

The sliding fixture prototype consists of a remotely actuated titanium pad (a copy of that welded on the cavity helium vessel) moving between two rolling needles arrays. Both stainless steel and titanium runners have been tested, the load being controlled through a spring washer set. Measurements have been performed with different surface roughness and the results compared and discussed.

The test apparatus is assembled in a stainless steel vacuum chamber which is part of the insert of a vertical cryostat that can be filled by liquid nitrogen or liquid helium. The vacuum system is designed to allow a controlled venting of the vacuum test chamber with different gasses and pressures. Ice effect on the sliding surfaces has been produced and its influence on the system performance has been measured.

To read the applied force, a commercial low cost load cell (from Philips) has been chosen and its measured characteristic curve is presented in Fig. 3. Its linear range reaches more than 10 kg_f, with a few gram accuracy and an elastic constant of 72.5 kg_f/mm. In our friction measuring system we chose a working point close to the center of the load curve, by means of applying an external weight to the actuation rod.

The motorized linear actuator uses a slide guide and is controlled by a programmable PID. The position is read with micrometric precision, while the velocity and acceleration are set via computer. In order to compensate pre-load effect on the reading of the load cell, a calibration has been performed on the basis of the data from a set of four different movement patterns and kinetic parameters. The settings used are summarized in Table 1. The movement shape can be easily deduced also from the time domains plot as shown in Fig. 4.

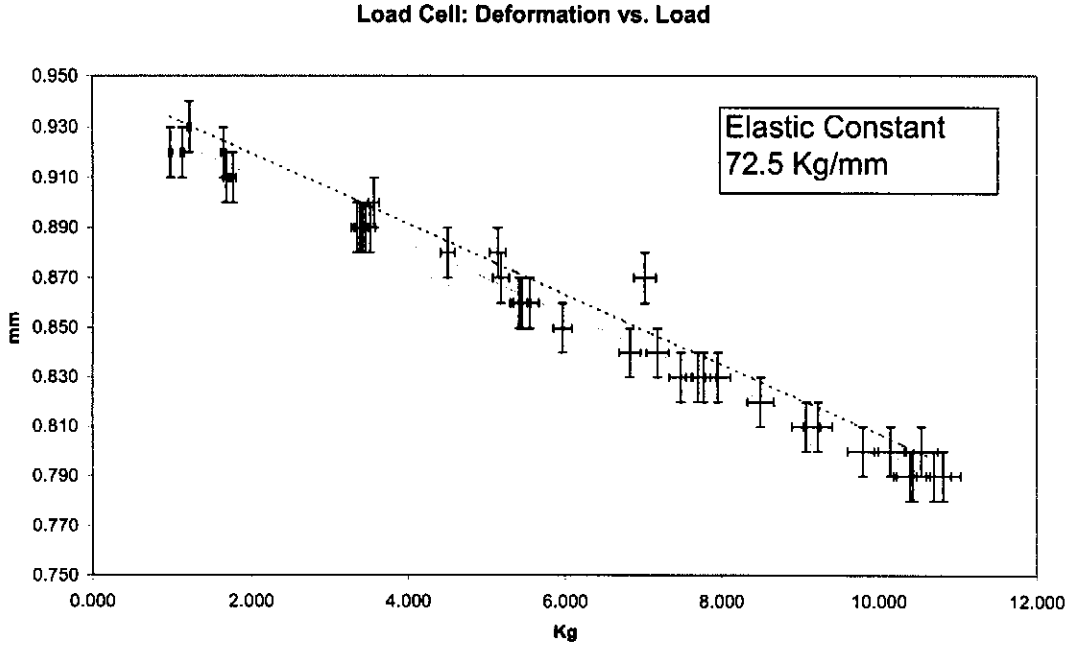

Figure 3. Displacement vs. force characterization of the load cell. The device shows a good linearity and reproducibility, with an elastic constant of 72.5 kg_f/mm.

Table 1. Actuator settings for the four different movement patterns used for calibration. They are obtained combining two velocity and acceleration sets with two motion types: I) 5 mm up, wait, 5 mm down; II) 2.5 mm up, wait, 2.5 mm up, wait, 5 mm down.

Pattern type	Velocity [mm/s]	Acceleration [mm/s^2]	Wait time [s]	Movement Pattern
1	0.25	0.25	5	I: Up 5 mm Wait Down 5 mm
2	0.25	0.25	2	II: Up 2.5 mm Wait Up 2.5 Wait Down 5
3	0.5	0.5	10	I: Up 5 mm Wait Down 5 mm
4	0.5	0.5	10	II: Up 2.5 mm Wait Up 2.5 Wait Down 5

DATA ANALYSIS AND INTERPRETATION

The system composed by the sliding pad, the runner, the rolling needles and the load cell is driven by the laws of static and dynamic friction. To describe and simulate this system we have developed a dynamic non linear numerical simulation. By exploring the parameter ranges of the model we have tested different movements setting, and chosen the movement patterns and parameters listed in Table 1, in order to allow a good sensibility to the static and dynamic friction effects. Fig. 4 summarizes some simulation results showing the difference in movement patterns of type I and II. This analysis predicts that the maximum extension of the signal from the load cell is equal two times the static friction, while the oscillation amplitude is equal to two times the difference between the static and dynamic friction. Unfortunately experimental results are not as clear as the simplified model used for the simulations, because surfaces roughness, the acquisition system and the instrumentation introduce noise that needs to be filtered by repeating several times the measurements. To discriminate the amplitude of the oscillations, that depends from the value of static and dynamic friction, we had to fit result including a proper error estimate.

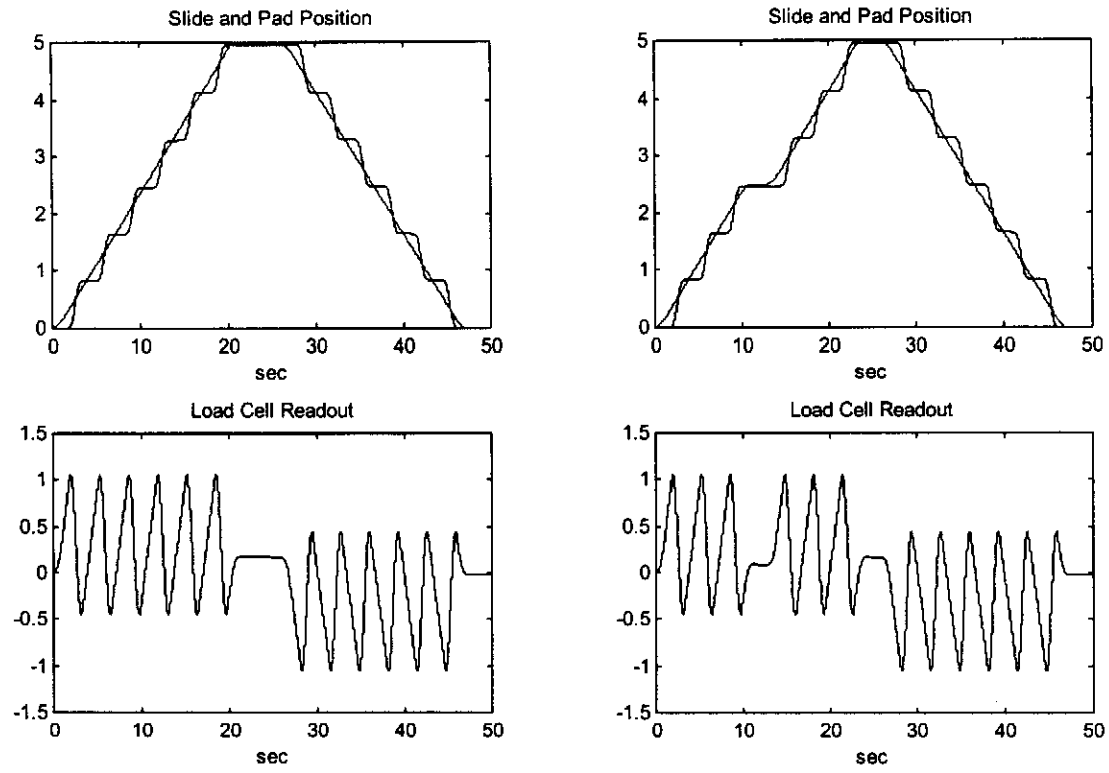

Figure 4. Simulated behavior of the readout system for movement patterns of type I (left) and type II (right).

MEASUREMENTS RESULTS

In order to qualify the cavity support system, stainless steel and titanium slides have been built and tested. The slides have been worked to a range of surface roughnesses, from very good to extremely rubbed, in order to test the starting life, end life and the case of extremely damaged components. Tests have been performed under different conditions of environment pressure, vacuum, and temperature. A failure in the vacuum system and the consequent surface icing has been also simulated. Each situation has been measured with the four movement patterns, each pattern has been repeat five to ten times, in the same slide position, with a very good repeatability to filter quantization noise. The same pattern has been then tested at different slide positions. An automatic LabView[4] procedure operated the movements and the data acquisition, while a Matlab[4] routine analyzed data and compute the measured static and dynamic friction, producing a report of the measured run (Fig 5 and Fig 6). All the four movement patterns (two sets for each pattern) are reported and plotted with the calculated friction value, and a summary comparing the eight measurements is generated. Using the eight results (of friction values and corresponding errors) a mean static and dynamic friction value is computed. The previous procedure has been repeated for the whole samples in the condition previously listed. Table 1 summarize the results acquired by the test system. The stainless steel slides have been used and tested also with a double force load (corresponding to about 80 kg_f), in order to check for the linear dependence of the measured friction values. The average friction force results in about 0.1 kg_f for stainless steel and about 0.8 kg_f for the titanium slide. The behavior of the

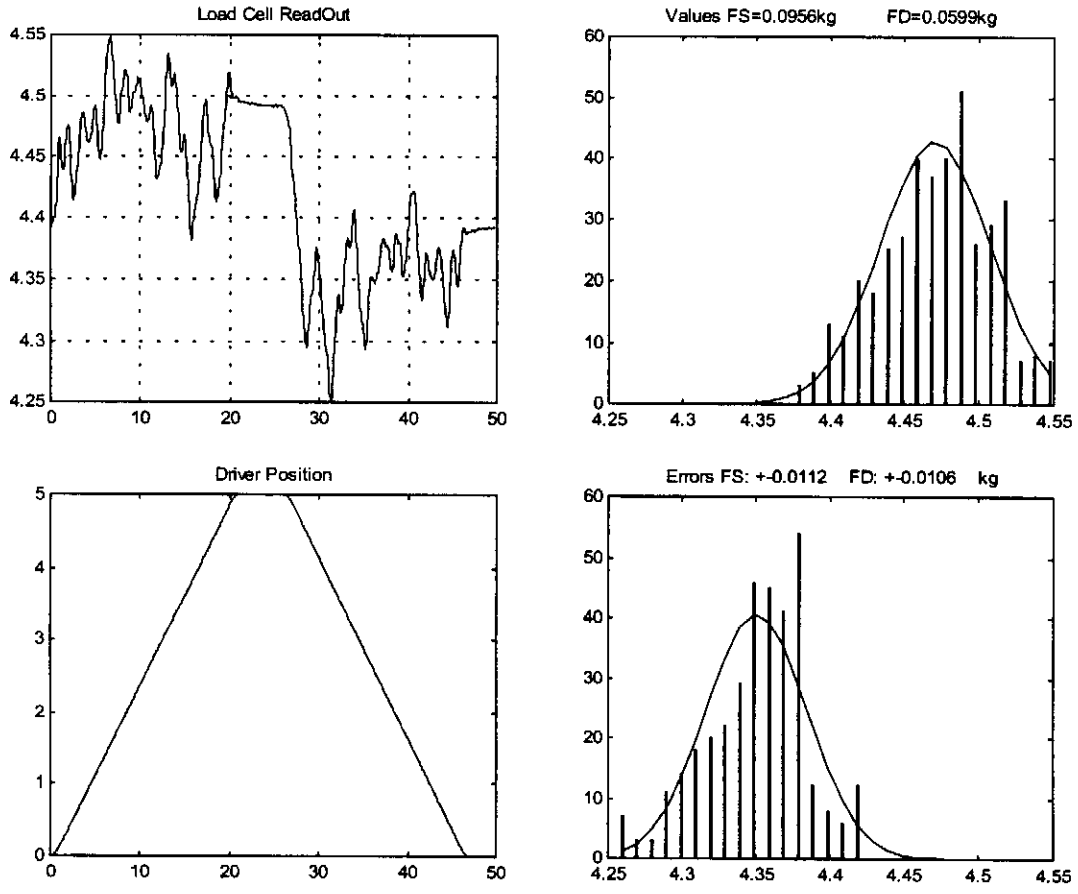

Figure 5. Data as output by the "Data Analysis Tool" developed to analyze the friction system results, for the case of the movement pattern of type I (Slow motion and single step). Studying the Load Cell tracks and checking them with the driving motor data the oscillations predicted by friction theory are reconstructed, and static and dynamic friction are evaluated, with their errors.

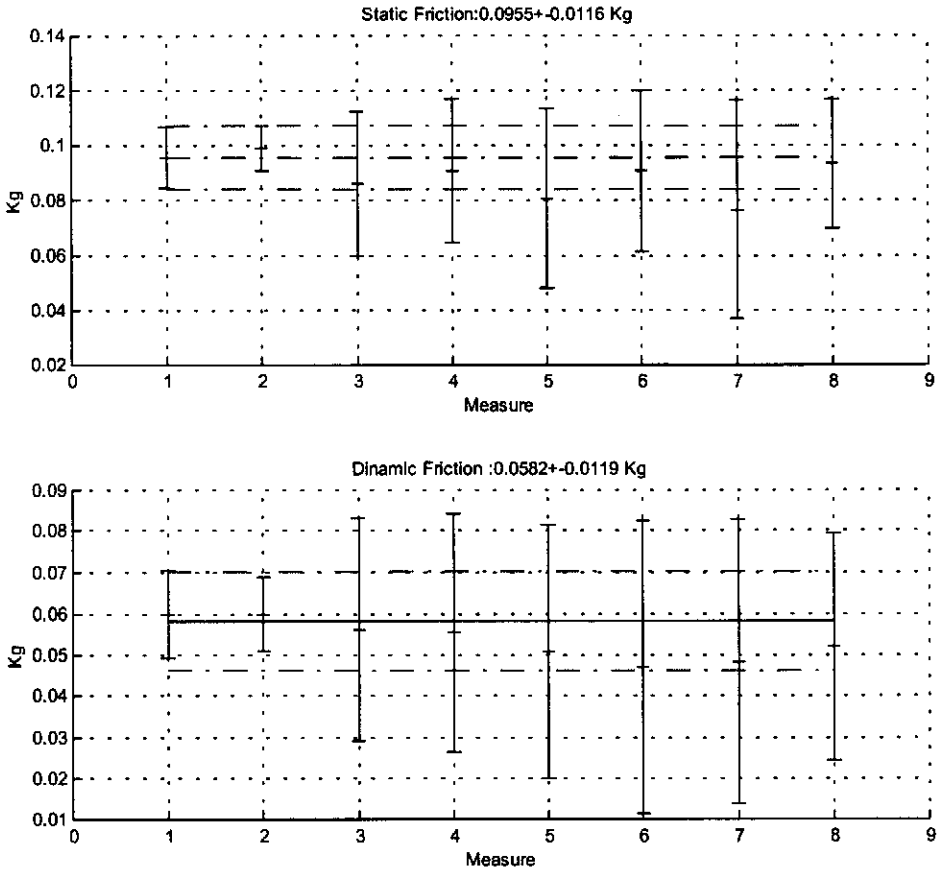

Figure 6. Results summary prepared by the "Data Analysis Tool". Results from the eight measures (four movement patterns, two run for each trip) are compared to achieve a final result value (and error) for dynamic and static friction.

slide does not depend strongly on the cryogenic temperature and no differences have been seen from the measurements. Icing effects have been "simulated" manually producing a vacuum break in the chamber at the liquid nitrogen temperature, raising the pressure to about 0.5 bar for 10 minutes (enough to condense water and other gases), but the rolling system performance was not impaired. The extremely damaged slides are characterized by an average friction value of about 0.8 kg_f, but some samples reached values up to 1.2 kg_f. This value is however compatible with the actual design of the cavities fixing feature[3] and should not be able to produce neither deformation in the cavity string nor damage in the supporting structure.

CONCLUSIONS

In this work the sliding support for SC cavities in long cryostats, proposed for the third generation of the TTF cryomodule have been qualified in its working condition. A test system has been built and used to simulate the cryogenic operation conditions of the support. Accurate data analysis has been necessary for the interpretation of the measurement results and to obtain static and dynamic friction in stainless steel and titanium sliding supports. A mechanical and vacuum failure has been simulated using severely damaged slides and icing the support during the test. Static friction measurements results in 0.1 kg_f reaction force with about 80 kg_f applied.

Table 2. Summary of the measurement results.

Sample[1]	Condition	Static Friction [kg_f]	Error [kg_f]	Dynamic Friction [kg_f]	Error [kg_f]
SS18	Liq. Nitrogen	0.0942	0.0266	0.0491	0.0203
SS18	Atm	0.0643	0.0078	0.0385	0.0061
SS18	Vacuum	0.0569	0.0135	0.0346	0.0118
SS36	Liq. Nitrogen	0.0901	0.0121	0.0449	0.0108
SS36	Ice	0.0715	0.0314	0.0362	0.0279
SS36	Atm	0.0979	0.0036	0.0564	0.0037
SS36	Vacuum	0.0955	0.0116	0.0582	0.0119
SS36Dam[2]	Liq. Nitrogen	0.5631	0.0761	0.2807	0.0751
SS36Dam[2]	Ice	1.0259	0.0381	0.6943	0.0460
SS36Dam[2]	Atm	0.4302	0.0387	0.2501	0.0375
SS36Dam[2]	Vacuum	0.4527	0.0330	0.2568	0.0346
Ti18	Liq. Nitrogen	0.1738	0.0433	0.0892	0.0352
Ti18	Atm	0.0756	0.0206	0.0458	0.0200
Ti18	Vacuum	0.0835	0.0210	0.0537	0.0189
SS18	Helium	0.0427	0.0153	0.0315	0.0214

[1] The "sample" notation is 'SS' for stainless steel and 'Ti' for titanium. The number is the spring load over the rolling needles, where 36 correspond to about 80 kg_f.

[2] The samples with the 'Dam' suffix have been heavily damaged before the tests.

REFERENCES

1. TESLA Test Facility linac - Design Report, DESY Report, March 1995, TESLA 95-01.
2. Conceptual design of a 500 GeV e+e- linear collider with integrated X ray laser facility, R. Brinkmann et al., editors, DESY Report, 1997-048, 1997.
3. Pagani, C., Barni, D., Bonezzi, M., Weisend II, J. G Further Improvements of the TTF Cryostat in View of the TESLA Collider, Presented at this Conference.
4. LABVIEW and MATLAB are trademarks.

Presented at: ***1999 Cryogenic Engineering Conference****, Montréal, Canada, July12-16, 1999*

FURTHER IMPROVEMENTS OF THE TESLA TEST FACILITY (TTF) CRYOSTAT IN VIEW OF THE TESLA COLLIDER

C. Pagani[1], D. Barni[1], M. Bonezzi[1] and J. G. Weisend II[2],

[1]INFN Milano-LASA, Via F.lli Cervi 201, I-20090 Segrate (MI), Italy,
[2]DESY, Notkestrasse 85, D-22607 Hamburg, Germany.

ABSTRACT

The experience gained in the commissioning and operation of the first and second generation of the TTF cryostat lead to a new and improved design which should fit the requirements of the TESLA collider in terms of cost and performances. The redistribution of the components in the cryostat cross-section allows to reduce by 15% the vacuum vessel diameter and to use a standard 38'' pipe. The thermal shields has been adapted to fit the new vacuum vessel, while the finger-welding technique has become a standard. A higher stability of the quadrupole package position, in spite of the possible asymmetrical forces acting on the Helium Gas return Pipe (HeGRP) edges during pumping and cooldown, has been obtained moving the three posts position. To assure the possible use of rigid couplers and superstructures a sliding support scheme has been developed for cavities. In connection with a reference Invar bar it lets cavities to stay fixed and aligned while the HeGRP slides over them during the cooldown and warmup.

INTRODUCTION

The development of the TESLA[1] collider cryomodule has arrived to the third generation which gained from the commissioning and operation of the three cryomodules already assembled at DESY. The cryomodule contains 8 cavities and a superconducting quadrupole package, it must provide cavity support, alignment, cooling, thermal insulation as well as feed-through for RF power, instrumentation and connection to adjacent cryomodules or to the cryogenic supply lines.

The third generation cryomodule needs to fit the requirements for TESLA collider to prepare the cryomodule mass-production in term of costs, mechanical requirements and cryogenic performances.

To appear on: *Advances in Cryogenic Engineering*, Vol. 45
Plenum Press, New York

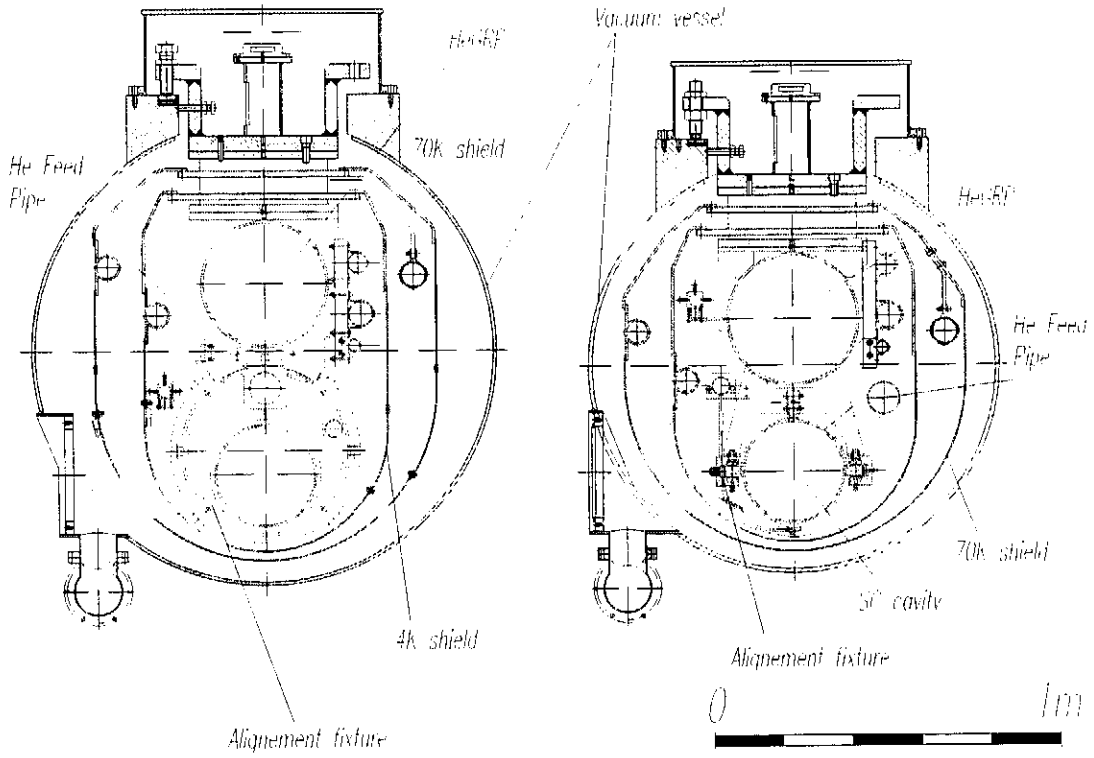

Figure 1. Comparison between second (left) and third (right) generation TESLA cryomodules. The components have been redistributed to fit the smaller vacuum vessel (38'' standard pipeline tube).

GENERAL LAYOUT AND CROSS SECTION

In order to improve the design of the third generation cryomodule an evaluation of each component and its influence in the general layout lead to the decision to use a standard pipeline tube for the vacuum vessel. Checking all possible solutions a 38 inches standard pipe (3/8''thick) has been chosen.

To arrange all components in the smaller vacuum chamber the thermal shields have been redesigned, filling the spaces and keeping margin to follow the tolerances on the standard pipe. The mayor improvement in the reduction of the cross section has been the decision to use an off-axis helium feed pipe. The requirements on superfluid helium distribution imposed to keep it above the helium tank level and below the gas return pipe. In this way the "off-axis solution" allowed the cavity axis to move closer to the HeGRP.

The new cavity support described in the following reduces also the space occupation in the lower region of the cross section, with respect to the previous design.

THERMAL SHIELDS

The cryogenic optimization of the TESLA module[1] string requires two thermal shield at 4.2K and at 70K. The shields are manufactured in aluminum (1050) and are both made of a roof (divided in two sections, each about 6 meters long) that supports eight panels. The panel length is 1.4 m, except for the first and the last. The shield panel length has been chosen in order to adjust the aluminum-stainless steel differential dilatation and to allow the coupler holes to follow the cooling cones.

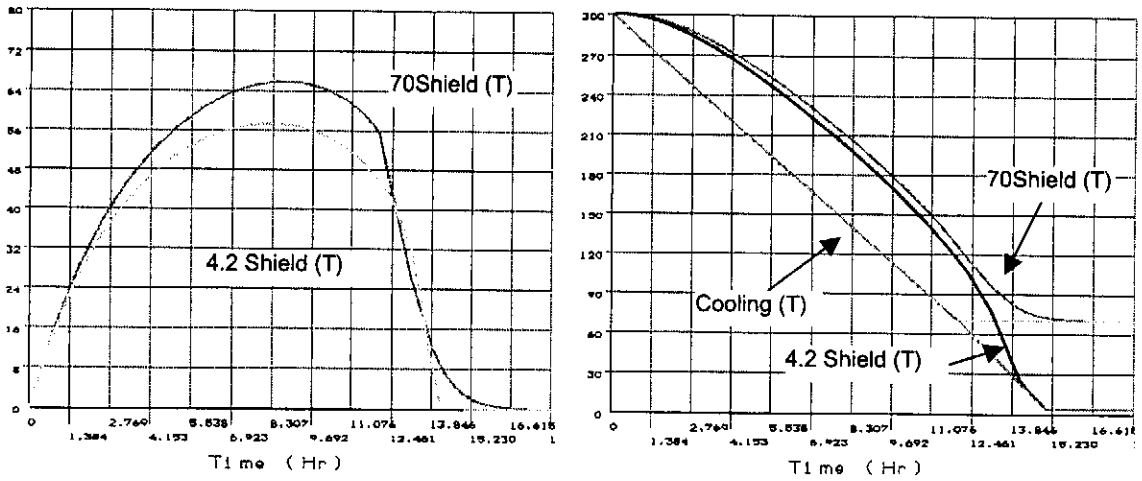

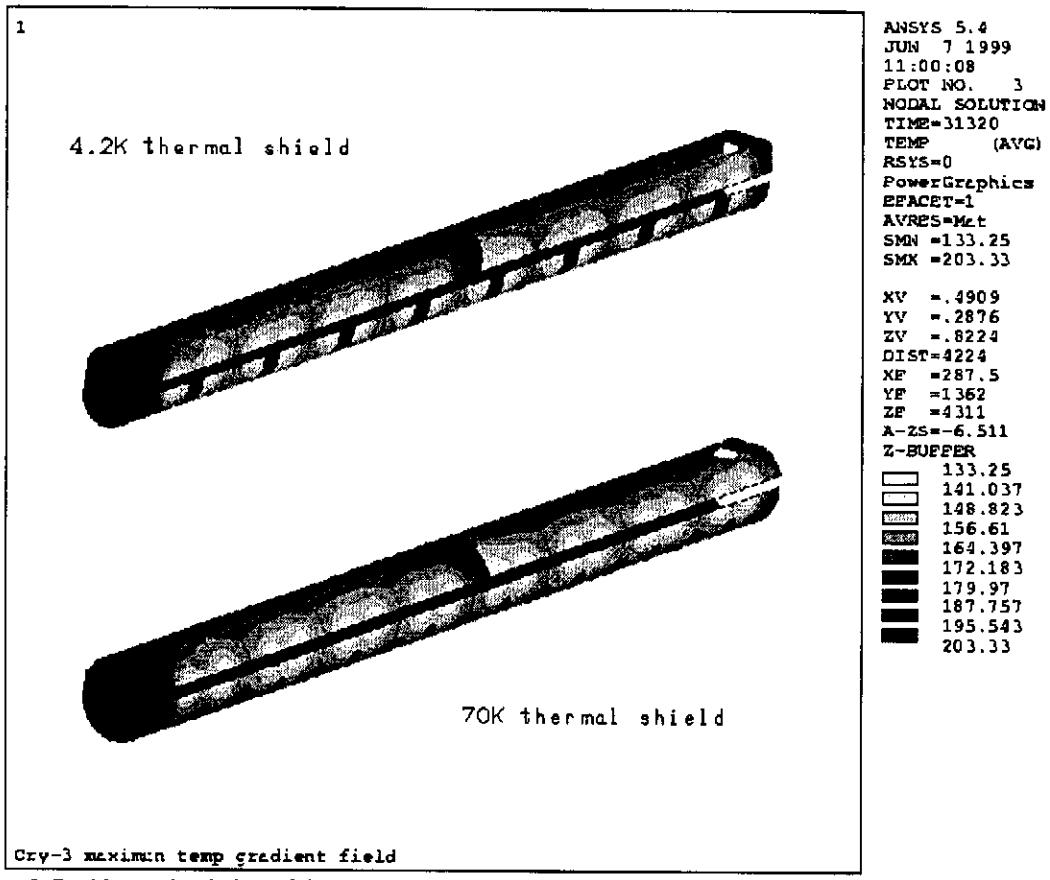

Figure 2. Cooldown simulation of the 4.2 K and 70 K aluminum thermal shields (upper right graph). We used a simultaneous 12 hour linear cooldown. The maximal thermal gradient on the shields (upper left graph) is below 60 K, a safe value. The temperature fields plotted in the lower figure show that the gradient is concentrated in the welding region, where the fingers unload the structure.

The shield cross-section have been adapted to the smaller vessel, with a rounder shape. The cooling pipe, as in second generation cryomodule, is an aluminum pipe, finger-welded[2] to the shield roof and to the panels. A bimetallic junction makes the transition to stainless steel in the connection region between cryomodules. The shield geometry has been checked by a finite element code to test for cooldown deformations and thermal inertia.

The results show that a 12 hour linear cooldown produces thermal gradients of about 60 K (Fig. 2) that induce deformations of ~10 mm (Fig. 4), which are compatible with the

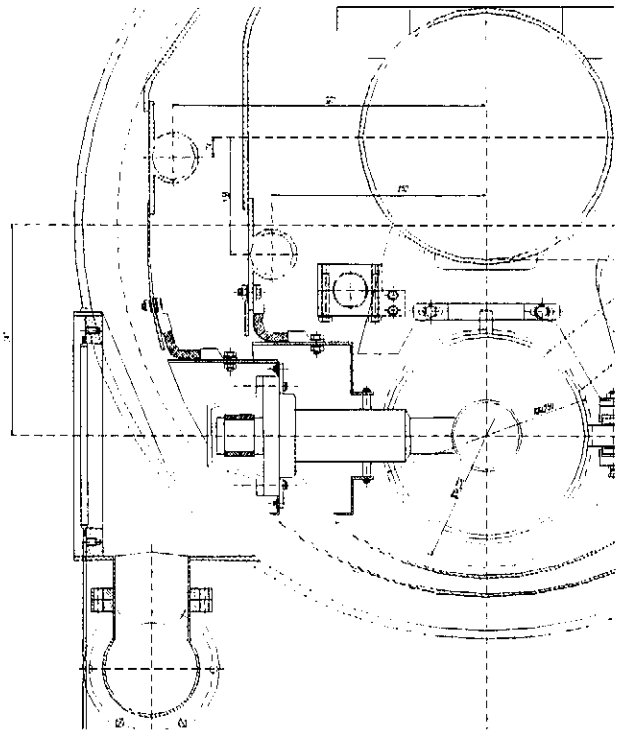

Figure 3. Coupler cones have been redesigned for an easiest fabrication and assembling. The cooling is guaranteed by copper braids connected to the shield panels.

geometric free space in the section. In order to ease the fabrication and to decrease the cost, the 6 meter shield roofs have been divided in two sections which are rigidly connected by screwed plates. This heat transfer discontinuity has been included in the model, in order to check its influence.

Using the temperature field calculated during the cooldown, a thermo-mechanical analysis has been performed in order to obtain the deformation and stress distributions in the aluminum shields. The results show a lateral bending of the shields, due to the asymmetric cooling ("banana" effect[3]) of about 10 mm, while the maximal stresses are within 30Mpa (the results are shown in Fig. 4).

Figure 4. Thermo-mechanical analysis of the shield panels. Applying the computed temperature field the deformations and stress distribution can be easily computed. The stresses (lower plot) are within 30 Mpa, while the deformation due to asymmetric cooling is below 10 mm (upper plot).

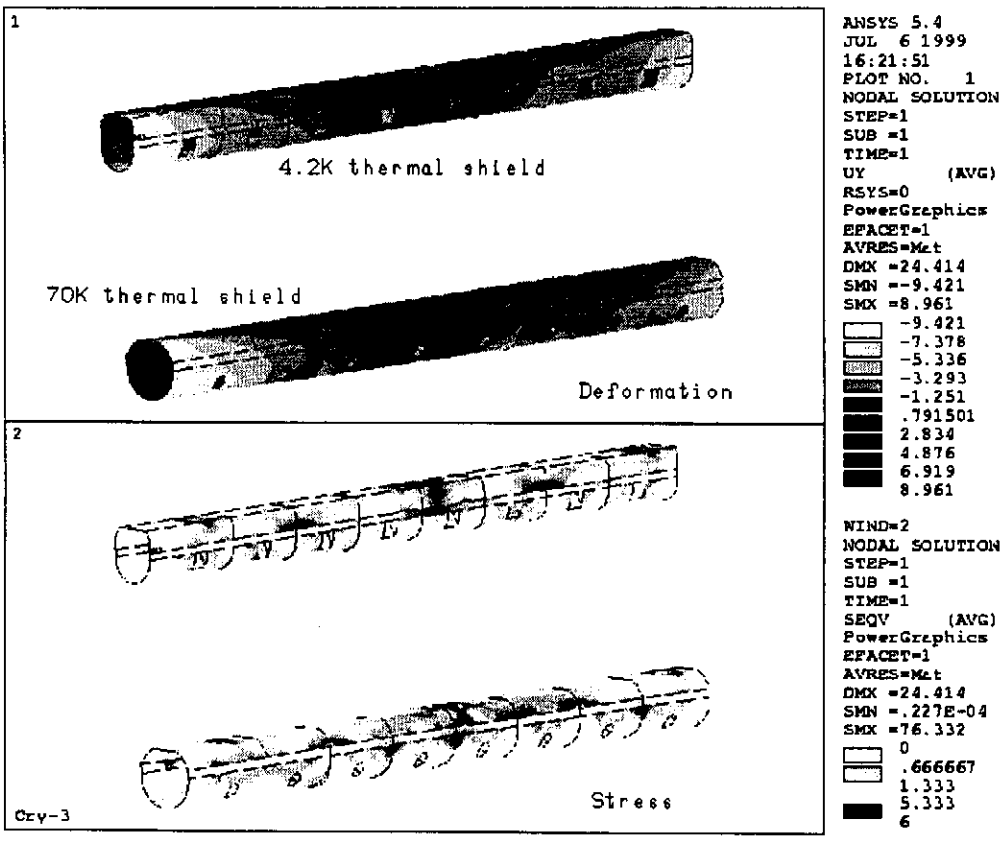

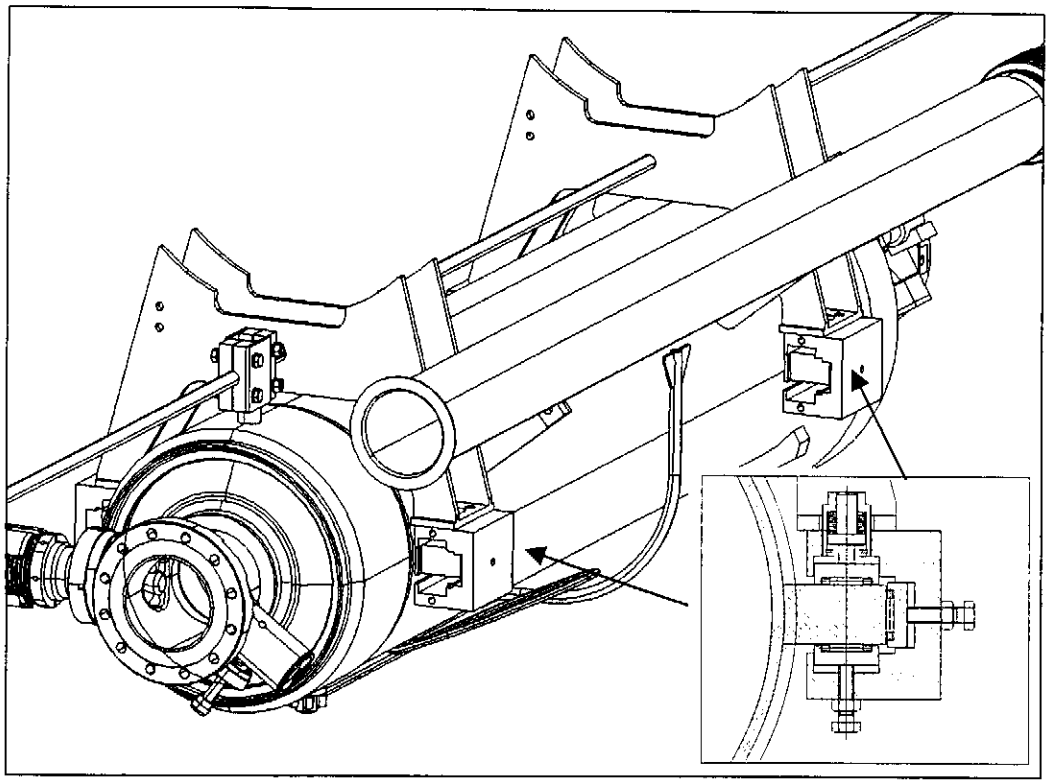

Figure 5. The cavity support system. Four C-Shaped stainless steel elements clamp a titanium pad welded to the helium tank by using rolling needles that reduce drastically the longitudinal friction, leaving cavities independent from the elongation and contraction of the HeGRP. Lateral and vertical position are defined by reference screws.

The shield panels and cooling pipes are used to cool other parts of the cryodomule. The post plates, which support the cold mass and the shield roofs, need to be kept at different temperature. In particular, the lateral post plates are connected to the shields with sliding supports which do not assure a good heat exchange. To achieve the post cooling, short and very flexible copper braids have been used. The same solution has been used for the coupler cones. The cones has been redesigned (Fig. 3) to ease the fabrication and the assembling. This solution has been, in part, already tested during the cooldown of cryomodule number two and sensors showed it worked correctly.

Table 1. Reference positions of the coupler port calculated for semi rigid coupler. The positions are relative to the fixed point. Hot to cold positions has been computed with Invar stainless steel and titanium relative contractions. The maximum displacement is less than 3 mm

Coupler N	1	2	3	4	5	6	7	8
External	-5113	-3733	-2353	-973	+407	+1787	+3167	+4547
Hot Position	-5113.5	-3733.5	-2353	-973	+407.5	+1768	+3168	+4548.5
Cold Position	-5122.3	-3732.8	-2352.9	-973.4	+406.5	+1786.5	+3165.9	+4545.9
Displacement	-0.5+0.7	-0.5+0.2	-0+0.1	-0+0.4	+0.5-0.5	+1.0-0.5	+1.0-1.1	+1.5-1.1

CAVITIES SUPPORTS

The experience in the assembling of the cryomodules #1, #2 and #3 [4] showed evidence that the cavity support system could be improved in terms of maintaining the cavity alignment. Due to the geometry of the system, it was too complicate to keep cavities

and quadrupole positions within the alignments requirements. The necessity to develop a system that could, in principle, be compatible with superstructure[5] or semi-fixed couplers lead to the decision of a complete redesign of the engineering of the cavity supports. The solution that has been proposed and studied needs to keep the cavity transverse position fixed, while leaving the cavity longitudinal position independent from the HeGRP thermal contraction and extension during the cooldown-warmup cycles. This objectives have been reached with a set of low friction sliding supports. The support, whose section is presented in Fig. 5, consists of a C-shaped stainless steel element that clamps a titanium pad welded on the cavity helium tank. The connection is mediated by a sequence of rolling needles, runners and reference screws. In each constrained direction (vertical and lateral) a reference screw defines the cold position of the cavity axis, and a spring washer package loaded at about 80 kg_f keeps the pad into contact. The friction between the cavity and the support has been measured and results in about 0.6 kg_f[6] This low friction value results in a decoupling of the cavity longitudinal position with respect to the supporting HeGRP. In order to be compatible with semi-rigid couplers and superstructures an Invar rod fixture determines the longitudinal position of the coupler ports. This solution results in a maximum total longitudinal motion of the coupler port of about 3 mm (Table 1 reports the computed hot and cold positions of each coupler port with respect to the external position).

COLD MASS SUPPORT AND COLD ALIGNEMENTS REQUIREMENTS

Analyzing the motion of the active elements during the cooldown of the cryomodule #1 and #2, as measured by the installed WPM[7] system, we have determined the presence of asymmetric forces in the feed-cap and end-cap sections of the module. This forces probably are generated by the misalignment of the HeGRP of the two consecutive modules, that deforms the HeGRP and moves the active elements out of alignment requirements. To reduce this effects two major improvements have been included in the present design. First

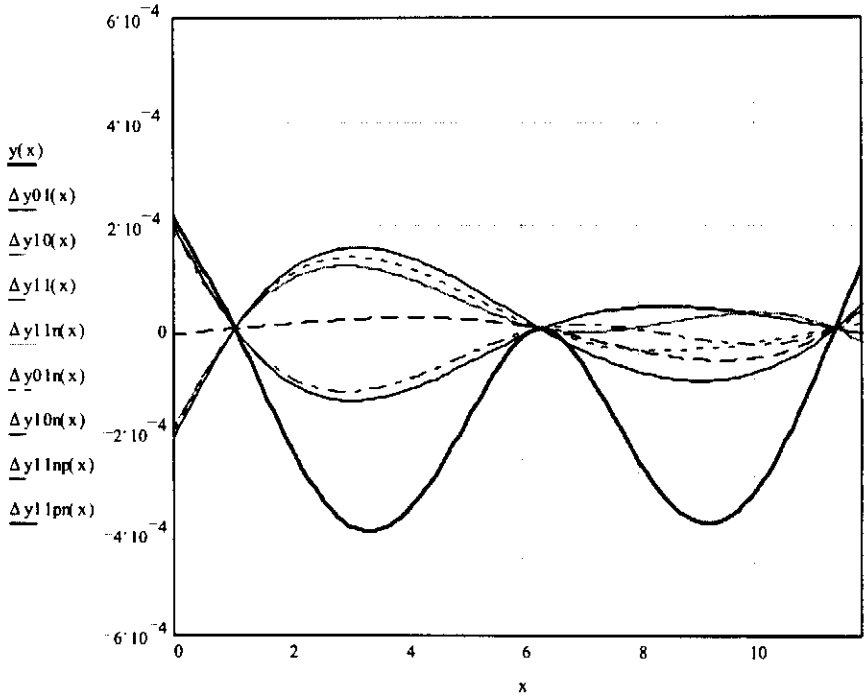

Figure 6. Computed deformation of the HeGRP when stressed by 1 KN asymmetric forces in the end cap and feed-cap position. The overall deformation is less then 0.2 mm in the cavities region and less than 0.1 mm for the quadrupole package. The solid line is the static absolute deformation with respect to cavities and quadrupole are aligned, while other lines are the displacements around the equilibrium position.

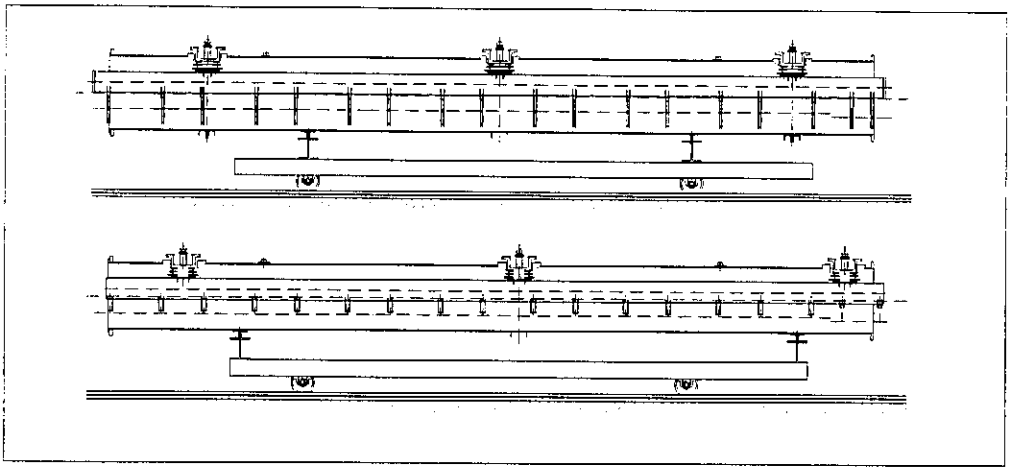

Figure 7. Comparison of second (upper) and third generation post positions (lower). The new solution improves the stability with respect to external unknown and asymmetric forces acting on the HeGRP and on the vacuum vessel during cooldown and under vacuum.

of all we changed the longitudinal positions of the support post. The most critical component, from an alignment point of view, is the quadrupole, so a support post has been placed over the fixture of the quadrupole package. The other two posts have been placed, compatibly with the assembling procedures, at positions that reduce the static deformation. To check this new solution a combination of 1 kN forces in all directions has been applied to the extremes of the HeGRP and the induced deformations have been computed. The displacement in the cavity region is within 0.2 mm in the worse situation, while at the quadrupole is estimated to be less than 0.1mm. In order to simplify further the design the support of the vacuum chamber has been modified. In the new design the same supports are used during assembling and in the linac operation. The positions have been chosen using the same philosophy of the HeGRP support, in order to minimize the reaction to unknown forces during operation. Figure 7 shows a comparison of the support positions in the second and third generation cryomodule. A support is very close to the quadrupole to minimize its possible movements, the other has been chosen with the compromise of a good stability and the space requirements during the assembly. Due to these changes all the assembling tools have been redesigned to fit the new geometry.

One other major improvement raises from the decision to include the bellow that links the HeGRP of two different modules in the fabrication of the HeGRP itself. This has increased the free space in the interconnection of the modules and has extended to the bellow flange the fabrication tolerances. The fabrication tolerances of the HeGRP are achieved by a 12 m milling machine that refers flanges and support element defining the axis of the tube. This operation can now be extended to the bellow flange. As a consequence the bellow is referred to the cryomodule axis and the connection between two consecutive HeGRP is more precise, and consequently less stressed. The result of this choice in the fabrication philosophy should be a sensible reduction of the external forces during pressurizing and cooldown.

The combination of the new support positions and fabrication process should achieve the cold alignment requirements for the cavities and the quadrupole package needed by the TESLA Collider Project.

CONCLUSIONS

We presented here the improvements introduced in the third generation of the TESLA cryomodule. The changes have been done in the direction of achieving the industrial mass-production requirements for the TESLA 500 Collider Project. The vacuum vessel has been reduced to a standard pipe (38''), the thermal shields have been redesigned to fit the space and to reduce the number of components. To insure a full compatibility with superstructures and semi-rigid couplers a new cavity support has been designed. A sliding fixture decouples the longitudinal motion of the cavities from the supporting HeGRP. In order to reduce the sensitivity to misalignments and to external forces the post and the vacuum vessel support positions have been changed. In this way the TESLA tolerances, especially in the quadrupole package region, should be matched.

REFERENCES

1. TESLA Test Facility linac - Design Report, DESY Report, March 1995, TESLA 95-01. Conceptual design of a 500 GeV e+e- linear collider with integrated X ray laser facility, R. Brinkmann et al., editors, DESY Report, 1997-048, 1997.
2. C. Pagani, D. Barni, M. Bonezzi, J. G. Weisend II, Design of the thermal shields for new improved TESLA Test Facility, Paper # FF 3, 1997 CEC/ICMC, Portland.
3. C. Pagani, D. Barni, M.Bonezzi, P.Pierini,J.G.Weisend II, Cooldown simulations for the TESLA Test Facility (TTF) cryostat, Paper # FF 4, 1997 CEC/ICMC, Portland.
4. J. G. Weisend II, C. Pagani, R. Bandelmann, D. Barni, A. Bosotti, G. Grygiel, R. Lange, P. Pierini, B. Petersen, D. Sellmann, S. Wolff, The TESLA Test Facility (TTF) Cryomodule: A Summary of Work to Date, Paper #CCB1, 1999 CMC/ICMC Montreal.
5. J. Sekutowicz, et al., Superconducting Super-structures for the TESLA Collider, Proc. of EPAC'98, Stockholm, Sweden, June 1998 and Desy Report, TESLA 98-08.
6. D. Barni, M. Castelnuovo , M. Fusetti, C. Pagani and G. Varisco, Friction Measurements for SC Cavity sliding Fixture in Long Cryostat, Paper #CCA3 , 1999 CMC/ICMC, Montreal.
7. D. Giove, A. Bosotti, C. Pagani, G. Varisco, A Wire Position Monitor (WPM) system to control the cold mass movements inside the TTF cryomodule, PAC97, Vancouver.

Presented at: ***1999 Cryogenic Engineering Conference***, Montréal, Canada, July12-16, 1999

The TESLA Test Facility (TTF) Cryomodule: A Summary of Work to Date

J. G. Weisend II [1], C. Pagani [2], R. Bandelmann[1], D. Barni[2], A. Bosotti[2], G. Grygiel[1], R. Lange[1], P. Pierini[2], B. Petersen[1], D. Sellmann[1], S. Wolff[1]

[1] Deutsches Elektronen-Sychrotron, DESY
Notkestrasse 85, 22607 Hamburg, Germany

[2] INFN Milano- LASA,
Via F.lli Cervi 201, I-20090 Segrate (MI), Italy

ABSTRACT

The proposed TeV Superconducting Linear Accelerator (TESLA) is a 30 km long electron / positron collider. The cryomodule is one of the principal building blocks of TESLA. The cryomodule contains the superconducting RF cavities that accelerate the beam along with superconducting focusing quadrupoles and associated cryogenic piping and thermal shielding. The cryomodules must meet strict requirements for alignment, heat leak vibration and cost. Approximately 2500 of these cryomodules are required for TESLA 500. Since 1997, three prototype cryomodules (of two different designs) have been built and tested in the TESLA Test Facility linac. This paper sums up the design, construction and operating experience with these prototypes. Measurements of alignment, heat leak and vibration of both designs are reported. The installation and performance of the new style thermal shields on the second prototype design are compared to the shields on the first prototype as well as to computer model predictions. Future cryomodule designs, allowing for fixed power couplers, are also discussed.

INTRODUCTION

An important aspect of the ongoing TESLA [1] project is the development of the cryomodules. Since 1997, a total of three cryomodules representing two different designs have been built and tested in the TESLA Test Facility Linac. The purpose of this paper is to summarize the experience with these prototypes and indicate the future direction of TESLA cryomodule design.

Role of the Cryomodules in TESLA

To appear on : *Advances in Cryogenic Engineering*, Vol. 45
Plenum Press, New York

The proposed TeV Superconducting Linear Accelerator (TESLA) is an electron / positron collider roughly 30 km long. The accelerating portion of the machine is built up of cryomodules. Each module contains 8 superconducting niobium cavities cooled to 2 K. Many modules also contain a superconducting magnet package consisting of quadrupoles and steering dipoles. The modules provide support, alignment and thermal shielding for the cavities and magnets as well as feed throughs for the RF power and instrumentation. The cryomodule is the fundamental building block for the TESLA machine. Approximately 2500 cryomodules are required for TESLA. These modules must meet strict requirements for alignment, heat leak, vibration and cost.

Cryomodule Requirements

Alignment. In order for TESLA to function properly as both a collider and a FEL driver, the cavities and magnets must be aligned to within certain tolerances. These tolerances must be maintained throughout transport, vacuum pumping and thermal cycling. For reasons of cost and complexity, there is no plan to allow adjustment of individual cavities once the module is assembled. Table 1 lists the alignment tolerances for the TESLA cryomodules. The axial tolerance is parallel to the accelerated beam while the transverse tolerance is in the plane perpendicular to the beam.

Static Heat Leak. As a superconducting RF device, the majority of the cryogenic load in TESLA comes from the RF power. However, the size of TESLA dictates that the static heat leak into the cryomodules also be kept as small as reasonable. Table 2 gives the expected static heat leaks at the 2 K, 4.5 K and 70 K levels.

Movable Couplers. The fixed point of the cryomodule is at the center. Thus the ends of the 12 m long module move 15 mm towards the center during cool down. This leaves the designer with a choice. Either fix the power couplers (and thus the cavities) with respect to the 300 K vacuum vessel and let them move relative to the rest of the cold mass or fix them to the cold mass and design the coupler to move relative to the 300 K vacuum vessel. Early on in the TESLA project it was decided to take the second option (that of movable couplers). Couplers [2] have been designed to meet these requirements. It may however be preferable to use fixed couplers and the third generation cryomodule design in principle permits the use of both fixed and movable couplers.

Vibration. Excessive vibration can affect the cavity tuning and resulting beam performance. The cryomodule should be designed to reduce the vibration to the cavities and magnets. The resonant frequency of the cryomodule should be far away from the 10 Hz repetition rate of the accelerator.

Table 1 Alignment Tolerances for TESLA Cryomodule

Component	Transverse tolerance	Axial tolerance	Rotational tolerance
Cavity	+/- 0.5 mm	+/- 5 mm	-
Quadrupole	+/- 0.1 mm	+/- 5 mm	0.1 mrad

Table 2 Predicted TESLA Cryomodule Static Heat Leaks

Temperature Level	Predicted Static Heat Leak (W)
70 K	76.8
4.5 K	13.9
2 K	2.8

Cost The size of TESLA dictates that the cost of each cryomodule must be kept as low as possible. While there is not a specific goal, reducing the cost of the cryomodule has been a consideration from the beginning. This has lead to the design of long cryomodules to minimize the number of expensive interconnects. Cost was the principal reason for changing the thermal shield design between cryomodule #1 and cryomodule #2.

CRYOMODULE DESIGN

1st Prototype

The cryomodule is 12 m long and contains 8 superconducting RF cavities. All cryomodules built so far also contain a superconducting quadrupole and steering dipole package. The cavities are bath cooled by saturated He II at 2 K. The cavity baths are supplied by a parallel two-phase He II line. The heat deposited in the He II evaporates vapor at the surface of the two-phase line and the resulting helium gas is returned to the refrigerator via a large diameter (300 mm) gas return pipe. The gas return pipe and two-phase line are connected together at the end of each module. The superconducting magnets are cooled by a separate 4.5 K flow. The same flow also cools the 4.5 K thermal shields. A second set of shields is cooled by a separate 70 K flow. The cryomodule also contains multilayer superinsulation (MLI) blankets on the 4.5 K and 70 K thermal shields and a separate warm up / cool down pipe parallel to the cavity string. All process lines are contained within the cryomodule.

Figure 1 shows a cross section of the first prototype cryomodule. The outer diameter of the vacuum vessel is approximately 1.2 m. The cavities and quadrupole package are directly attached to the 300 mm gas return pipe. This pipe is itself attached to the 3 composite support posts arranged axially along the length of the module. The middle post is fixed. The 2 outer posts along with the 300 mm pipe, cavities, magnets and shields move towards the center of the cryomodule as a result of thermal contraction during cool down.

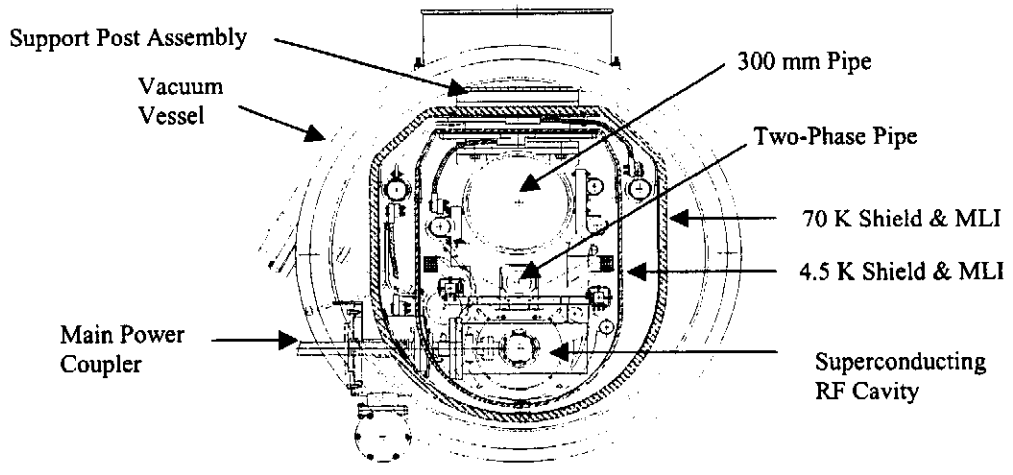

Figure 1 Cross section of 1st prototype cryomodule

The gas return pipe is the structural backbone of the cryomodule and is key to the alignment of the cavities and quadrupole. The gas return pipe is aligned relative to the ideal beam axis via adjusting screws on the support posts. The cavities and quadrupole are then each aligned relative to the ideal beam axis via adjustment screws attaching them to the 300 mm pipe. Once this is accomplished, the cavity alignment is determined by the pipe alignment. As long as the gas return pipe is in the proper position relative to the beam axis, the cavities will be as well. This design only works properly if the cavities don't move relative to the 300 mm pipe once aligned and the 300 mm pipe doesn't move in an unexpected manner once aligned relative to the beam axis. Upon cooling, thermal contraction will cause the 300 mm pipe, cavities and quadrupole to move vertically upwards by 1.8 mm relative to their warm position. This effect is allowed for in the alignment process.

In the first prototype cryomodule, the thermal radiation shields at 4.5 K and 70 K are constructed from aluminum and the cooling pipes are stainless steel. Large copper braids fastened between the shields and the cooling pipes cool the shields. Each thermal shield is divided into 18 pieces connected together by thread fasteners.

One example (cryomodule #1) of this first prototype design has been built.

2nd Prototype

The second prototype design is virtually identical to the first prototype with the exception of the thermal radiation shields. There were two problems with the initial shield design. First, the copper braids used to cool the shields were bulky, expensive and not completely reliable. Second, the use of threaded fasteners to connect the shield pieces together was very expensive in both material and manpower. To solve these problems, it was decided to cool the shields with aluminum cooling pipes that were directly welded to the shields. Welding was also used instead of fasteners to connect the shield pieces together. In order to prevent excessive stress and deformation of the welded joints during thermal cycling a finger welding technique was used. Extensive FEA modeling was performed [3] to predict the behavior of the new shield design. The use of welded shields does place limits on the cryomodule cool down rate, but these limits are consistent with those imposed to prevent excess deformation of the gas return pipe during cool down.

Based on the experience of cryomodule #1, the mechanical tolerances of the second prototype design were adjusted. Those tolerances that were tighter than necessary were relaxed and the reference points of all the tolerances were adjusted to better match the manufacturing and assembly process.

The changes to the thermal shield design and the tolerances resulted in a cost savings of almost 50 % for the cold mass (that is everything except the cavities, quadrupole and their related components) between the first and second prototype design. Two cryomodules (cryomodules #2 and #3) were built to this second prototype design.

CRYOMODULE ASSEMBLY

So far, 3 cryomodules have been assembled at DESY. The assembly process begins when the assembled string of eight cavities and one quadrupole is removed from the clean room. The two-phase He line connecting the cavities is then welded and leak checked. Next MLI, magnetic shields and temperature sensors are added to the cavities. The cold mass (provided by INFN) is then placed on the assembly tooling above the cavity string. The three support posts of the cold mass are adjusted so that the 300 mm gas return pipe is level straight and aligned with the reference beam axis. The cold mass is then carefully lowered onto the cavity string and attached to it. The resulting assembly is then lifted off the string

support carts. A precision screw gear linkage system in the assembly tooling permits this to be done with damaging the cavities. Next the cavity tuner linkages and motors, remaining sensors, cables and magnetic shielding are installed. The system is now ready for final alignment.

The alignment is one of the most critical steps in the assembly. Each cavity and the quadrupole are aligned to the reference beam axis using adjustment screws that connect them to the cold mass. Experience showed that tightening the supports after the alignment in some cases altered the alignment. Thus, it is necessary to measure the alignments after the supports are tightened and realign the components as needed. In cryomodules #1 and #2 the alignment was not done to within the required tolerances to avoid damaging the cavities. However, in assembling cryomodule #3, all the components met the final alignment tolerances. The alignment takes 3 days.

After the alignment is finished, the beam tube vacuum is leak checked and the cryomodule is moved to another assembly position. Here the 4.5 K thermal shields, 4.5 K MLI, the 70 K thermal shields and 70 K MLI are installed. Temperature sensors are installed as needed on the thermal shields. Next the 300 K vacuum vessel is slid over the cold mass and attached to it via the support posts. The support posts are then realigned to bring the gas return pipe (and thus the cavities and quadrupole) back into alignment with the ideal beam axis. Lastly, the warm parts of the main couplers, the quadrupole current leads and all the instrumentation feed throughs are installed. The cryomodule is now ready for installation in the linac.

The assembly of the welded thermal shields used in cryomodules #2 and #3 went very well. One team of two welders was able to install all the shields of a module in less than 2 days. No damage was done to any of the cryomodule components during the welding.

Eight weeks were needed to assemble cryomodule #1. Cryomodule #2 and #3 each required 6 weeks. Additional time savings should be possible in the future with elimination of the sensors now needed for research and some automation of the assembly process.

OPERATING EXPERIENCE

Introduction

Two cryomodules (CM #1 and CM #2) have been cooled down and operated with RF power and beam. Cryomodule #1 has been in operation since June 1997 and has undergone 5 thermal cycles. Cryomodule #2 was first cooled down in November of 1998 and has undergone 2 thermal cycles. The performance of the cryomodules was measured during these experiments.

Heat leak

The static heat leak to the 70 K and 4.5 K levels was found by measuring inlet and outlet temperatures and pressures, calculating the change in enthalpy and multiplying by the measured mass flow rate. Measurements with test heaters wrapped around the 70 K and 4.5 K cooling lines indicate that the error in these measurements is less than a few percent. The 2 K result was calculated by multiplying the latent heat of helium at 2 K times the measured vapor mass flow rate at the vacuum pumps; after subtracting out the amount of vapor generated during the J-T expansion at the inlet to the two-phase line.

Table 3 compares the predicted and measured static heat for the two cryomodules. Note that there are two sets of results given for cryomodule #1. When cryomodule #1 is operated alone, the end of the cryomodule is connected to a special cryostat known as the

Table 3 Static Heat Leak Results

Temperature Level	Predicted Heat Leak (W)	Measured Heat Leak (W) Cryomodule #1 (alone)	Measured Heat Leak (W) Cryomodule #1 (with #2)	Measured Heat Leak (W) Cryomodule #2
70 K	76.8	90	81.5	77.9
4.5 K	13.9	23	15.9	13
2 K	2.8	6	5	4

Endcap. When cryomodule #1 and #2 are operated together the end of cryomodule #1 is connected to cryomodule #2 via 12 m long bypass transfer line. This transfer line is simpler in function than the original endcap and causes less heat leak to cryomodule #1. In particular, the old end cap contained optical windows which penetrated to the 2 K space and added heat to both the 4.5 K and 2 K levels. The absence of these windows is seen in the data. The heat leak in cryomodule #2 is smaller than that of cryomodule #1 and closer to the predicted values. This results from the smaller number of sensors in cryomodule #2 and a corresponding reduction in heat leak due to instrumentation cables.

Performance of new shield design

Figure 2 shows the measured temperature distributions on the 4.5 K and 20 K shields in cryomodule #2. The shields performed quite well. The temperature at each level is quite uniform and the temperature of the shield is within a Kelvin or two of the desired level. No damage was done to the shields during the controlled cool down and warm up of the cryomodule. The results here are consistent with the FEA predictions [3]. In particular, the temperatures on either side of the predicted thermal neutral line (180° from the cooling pipe) are equal as expected. The 8 K and 9 K temperatures at the end of the 4.5 K shield are most likely a result the heat sinking of wires to the shield in that region.

The performance of the new shields in cryomodule #2 shows that the simpler, less costly design will meet the cryomodule requirements.

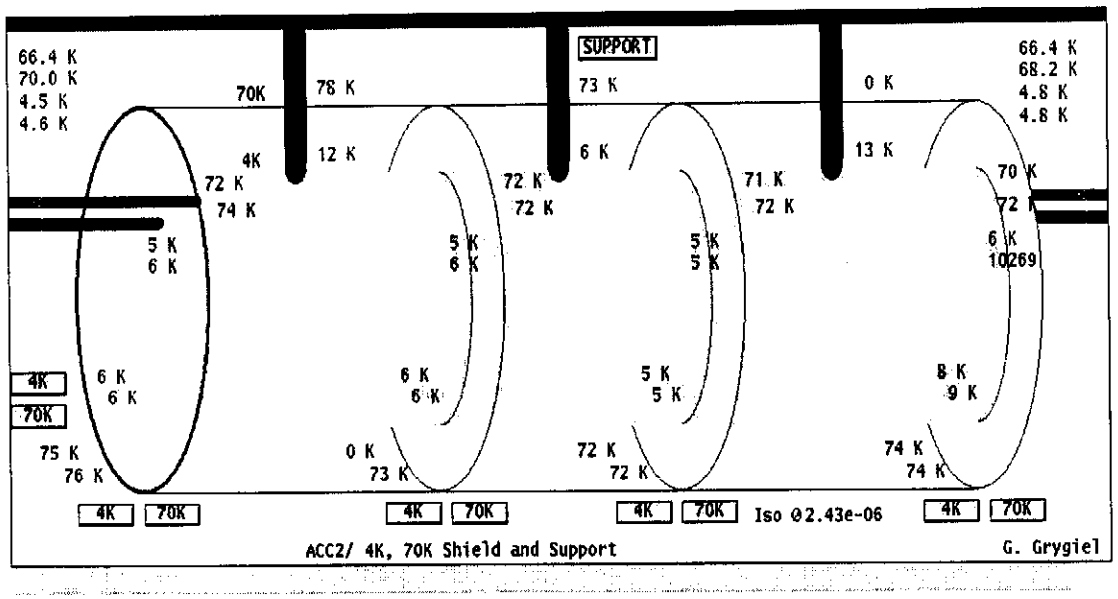

Figure 2 Measured temperature distributions on the 4.5 K & 70 K shields for cryomodule #2

Alignment

The change in the alignment of the cavities and quadrupole is measured by a wire position monitor system [4] produced by INFN. This system permits the real time measurement of position of the components with a resolution of 50 microns. Figures 3 and 4 shows the change in horizontal position for the cavities and quadrupole in cryomodules #1 and #2. Similar results are seen for the change in the vertical system. In these plots, the quadrupole is the rightmost data point. The remaining points represent cavity positions. Notice that the greatest deflection comes at either end of the cryomodules. This results from unbalanced forced generated on the 300 mm gas return pipe during vacuum pumping and cool down. These forces deflect the pipe and thus the attached cavities. Unfortunately, the quadrupole which has the tightest alignment tolerance (+/- 0.2 mm) is located at the end of the cryomodule. Thus, it is always out of tolerance. The cavities, by contrast, are almost always within their tolerance of +/- 0.5 mm. Note also, that the 300 mm pipe does not return to its original position after being warmed up. Some residual forces remain. While the changes in the quadrupole position do not effect the performance of the TTF linac they will be too large for proper performance of the TESLA 500 machine. One of the changes in the 3rd generation cryomodule is designed to solve the alignment problems.

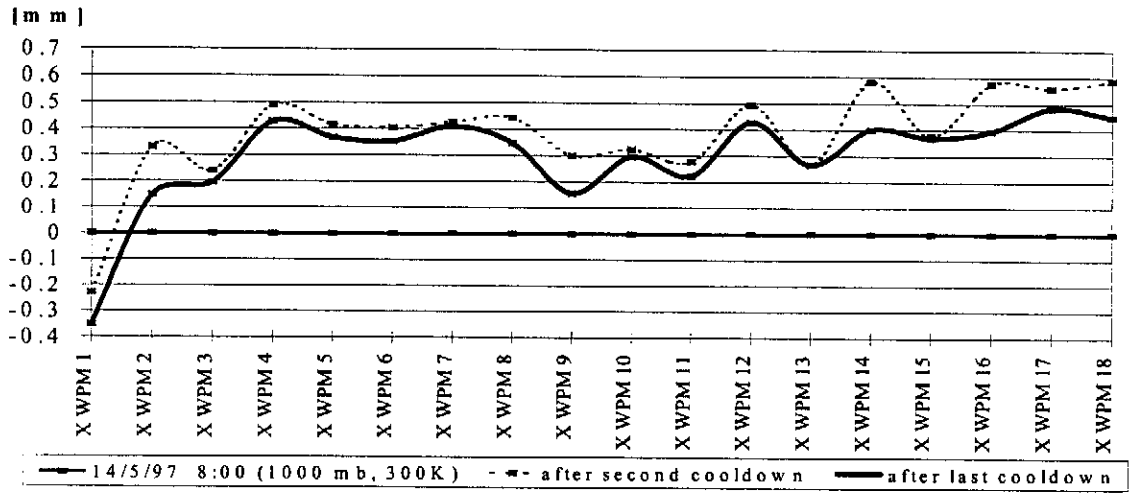

Figure 3 Horizontal displacements of the cavity string for Cryomodule #1 as measured by the WPM system

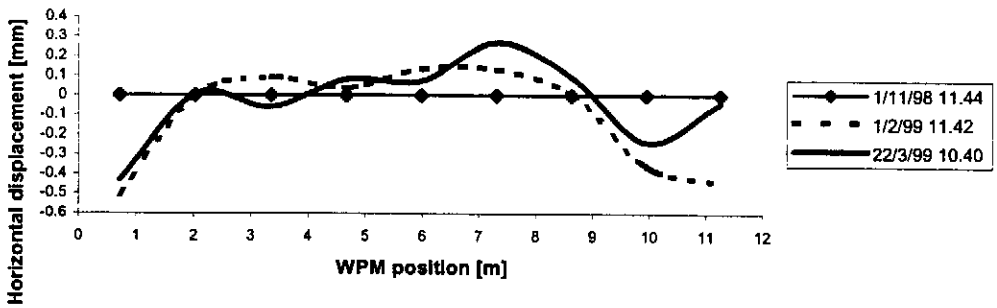

Figure 4 Horizontal displacements of the cavity string for Cryomodule #2 during cooldown (1/2/99) and warmup (22/3/99) compared to the original position (1/11/99)

Vibration

The best test of the cryomodule's resistance to vibration is operational. Excessive vibration will result in a detuning of the cavities off their resonant frequencies or perhaps in beam jitter and defocusing. None of these effects have been seen during several years of operation despite the cryomodules operating over a range of helium flow rates and heat loads. The cryomodules thus meets the vibration requirements.

3RD GENERATION DESIGN

Based on the results from the first two generations of cryomodule design, a 3rd generation design has been developed. This new design:

- Reduces the outer diameter of the cryomodule from 1.2 m to 0.98 m. This was accomplished by changing the connection of the cavities to the cold mass and by slightly moving the two-phase pipe. The smaller size frees up room in the proposed TESLA tunnel.

- Stiffens the 300 mm tube near the quadrupole by moving the support posts . Analysis shows that this should permit the quadrupole to stay within its alignment tolerance with unbalanced forces of up to 1000 N

- Allows the use of rigid or semi-rigid main couplers by connecting the cavities to the cold mass by a series of roller bearings and a parallel Invar rod. This may result in significant cost savings for the main coupler as well as an easier and less expensive cryomodule assembly procedure

- Uses the improved thermal shield design tested in cryomodules #2 and #3.

Figure 5 shows a cross sectional view of the new design. The first of these new cryomodules should be built at the end of 1999. More details about the design are presented elsewhere in this conference[5]

Figure 5 Cross section of the 3rd generation cryomodule design

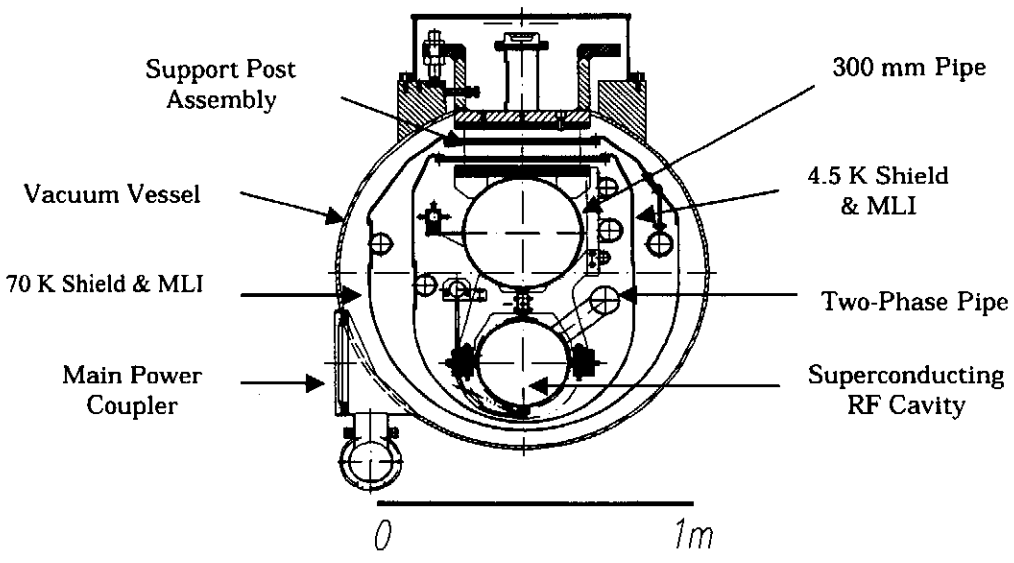

SUMMARY

In the past 5 years, significant progress has been made in the development of cryomodules for TESLA project. 3 cryomodules representing 2 different designs have been constructed. By changing the thermal shield design and adjusting the mechanical tolerances, the 2nd generation cold mass is significantly less expensive than the 1st. Two of these cryomodules (one of each design) have been tested in the TTF linac. The results show that the design meets or comes close to meeting the requirements for vibration and heat leak. The alignment of the quadrupole tends to exceed the tolerances. In order to solve this problem as well as to reduce the outer diameter of the cryomodule and allow for the possibility of fixed power couplers, a 3rd generation design has been created.

REFERENCES

1. R. Brinkman, et al. eds. Conceptual design of a 500 GeV e+e- linear collider with integrated X ray laser facility ,DESY Report, 1997 –048 (1997).
2. K. Koepke, "Design of Power and HOM Couplers for TESLA", *Adv. Cryo. Engr.* Vol 41a, 877 (1996)
3. C. Pagani, D.Barni, M. Bonezzi, P. Pierini, J. G. Weisend II, "Design of the Thermal Shields for the New Improved Version of the TESLA Test Facility (TTF) Cryostat" *Adv. Cryo. Engr.* Vol. 43a, 307 (1998).
4. D. Giove,., et al., "A wire position monitor (WPM) System to Control the Cold Mass Movements Inside the TTF cryomodule, Presented at PAC 97, Vancouver, Canada (1997).
5. C. Pagani, D.Barni, M. Bonezzi, J. G. Weisend II, " Further Improvements of the TTF Cryostat in View of the TESLA Collider" Presented at 1999 Cryogenic Engineering Conference (Montreal).

Presented at: ***1999 Cryogenic Engineering Conference****, Montréal, Canada, July12-16, 1999*

STATUS AND PERSPECTIVES OF THE SC CAVITIES FOR TESLA.

Carlo Pagani for the TESLA Collaboration,

INFN Milano-LASA and University of Milano
Via Fratelli Cervi, 201, I-20090 Segrate (MI), Italy

ABSTRACT

To fulfill the requirements of TESLA, the superconducting option for future linear electron-positron collider, a TESLA Test Facility (TTF) is under construction and commissioning at DESY by an International Collaboration. In this framework an extensive R&D program started in 1992 at DESY, and worldwide in the different laboratories participating in the Collaboration, to establish a reliable and cost efficient technology to industrially produce 9-cell pulsed cavities, at 1.3 GHz, with accelerating field exceeding 25 MV/m. In this paper the outstanding results obtained so far, as demonstrated by vertical tests and operation in TTF at DESY, are shown. In addition the perspectives of further improvements emerging from new cavity fabrication and processing techniques under development by the Collaboration are presented.

INTRODUCTION

A high energy e^+e^- linear collider with a center of mass energy of 500 GeV and higher is considered an essential tool to search for fundamental constituents of matter and their interactions and to address the problem of mass generation in the Standard Model. Worldwide a number of groups are pursuing different design efforts towards a next generation TeV Linear Collider. The different accelerator designs can be divided in two main categories: the high frequency, room temperature approach (NLC, JLC, VLEPP & CLIC) and the low frequency, superconducting one (TESLA). The combination of high conversion efficiency from mains to beam power (17-23%), together with small emittance dilution in the low-frequency (1.3 GHz) superconducting linac, makes the last choice ideal for an optimum performance in terms of the achievable luminosity [1].

From the work started in 1990 [2], a concept of a 500 GeV centre-of-mass energy superconducting linear collider emerged, based on 9-cell cavities operating at 1.3 GHz. An accelerating field of 25 MV/m @ $Q=5\cdot10^9$ was envisaged, the expected luminosity being $5\cdot10^{33}$ cm^{-2} sec^{-1}. In 1991 several institutions decided to join the efforts in the TESLA Collaboration – formally established in 1994 – to set up at DESY the necessary infrastructure, while building a new generation superconducting linac, that is the TESLA Test Facility (TTF) [3]. At present, more than 30 institutes from Armenia, P.R. China,

To appear on: *Advances in Cryogenic Engineering*, Vol. *45*
Plenum Press, New York

Finland, France, Germany, Italy, Poland, Russia and USA participate in the TESLA Collaboration and contribute to TTF.

The conceptual design report (CDR) of the TESLA 500 GeV collider was published in May 1997 [4] giving a complete description of the machine, including all the subsystems. Due to the low RF frequency, which implies better emittance preservation, and the long macro-pulses, a superconducting linac based on the foreseen TESLA technology lends itself as the best choice for the driver of a X-ray Free Electron laser (FEL), working in the Self-Amplified Spontaneous Emission (SASE) regime. So that, a SASE FEL user facility has been included as an integral part of both TTF and TESLA projects [3,4].

With respect to the existing large-scale installations of superconducting cavities (e.g. LEP and CEBAF), the major challenge for the feasibility of a superconducting linear collider was to reduce the cost per unit energy gain (MeV) by more than an order of magnitude. This means both to reduce the cost per unit length and to increase the accelerating gradient by about a factor of five, to 25 MV/m and more.

THE TESLA TEST FACILITY (TTF)

The TESLA Test Facility (TTF) is under construction at DESY, with major components flowing in from the members of the TESLA Collaboration. Figure 1 shows the general layout of TTF Phase I, in Building 28 (Hall 3). It comprises the complete infrastructure for the treatment, assembly and test of the 9-cell superconducting cavities, and a superconducting linac, composed by 3 cryomodules with 8 cavities, for an integral test of the machine critical components. An average cavity gradient of 15 MV/m was the initial goal, as a first step to reach the design gradient of 25 MV/m required by TESLA.

TTF Phase I is now close to completion and Phase II is under construction. It will include 5 more cryomodules, of the final TESLA design [5], placed in a building extension simulating the TESLA tunnel. A 25 m long undulator will be installed ad the end of the linac by fall 2001, to feed a FEL user facility with photon energies up to 200 eV.

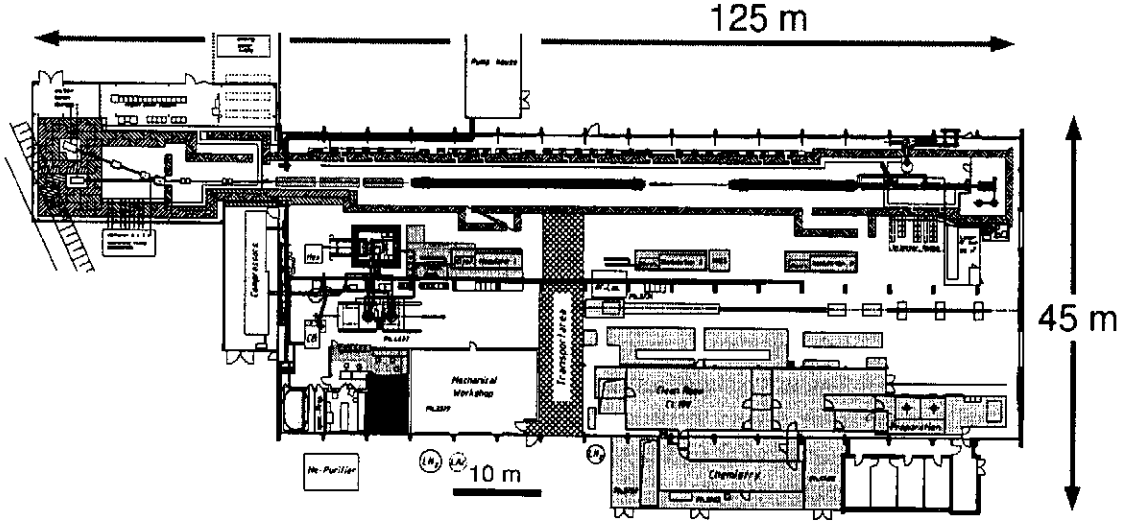

Figure 1. TESLA Test Facility linac (Phase I) and infrastructures at DESY. In the upper part, from right to left: injector, capture cavity, bunch compressor, first cryomodule, second bunch compressor, string of cryomodules #2 and #3, three undulator sections, beam analysis and dump. On the lower right: the cavity preparation infrastructures and the cryomodule assembly station. On the lower left: cryogenics and cavity cold test area.

The TTF linac

A 4 MeV laser-driven RF photoinjector [6] is producing the TESLA beam, that is a one millisecond long bunch train with an average current of 8 mA and a bunch charge of 8 nC. The electrons are then captured by a single 9-cell cavity to be injected in the first cryomodule at an energy of the order of 20 MeV. In 1997 the first cryomodule containing eight 9-cell cavities with an average gradient of 15 MV/m has been successfully commissioned while the second module was installed in summer 1998. An important step toward TESLA specs was made by achieving a minimum cavity gradient of 20 MV/m. Four cavities actually reached the TESLA goal (25 MV/m). The cavities of the third module, which has been recently assembled and will be cooled down by end of July, are expected to operate at an average gradient of 25 MV/m. This module is being installed in place of module # 1. The old module # 1, renewed in cryogenics and equipped with high performance cavities, will complete TTF Phase I by the end of the year. By August two modules together with photoinjector, capture cavity, bunch compressor and a 15 m long three section undulator will be operated for the SASE FEL proof-of-principle experiment. A beam energy up to 380 MeV will be available, the same as that originally foreseen for TTF Phase I with 3 cryomodules.

As stated above, we expect to conclude the installation of Phase II by fall 2001. The new generation cryomodules [5], which are smaller in diameter and allow for semi-rigid coupler and superstructures[9] are now in fabrication. The delivery of the first two is expected this year while a new batch of 24 cavities will be delivered starting January 2000.

The TTF infrastructures

The TTF infrastructure for cavity preparation and test[6], completely operational since the end of 1995, consists of a complex of clean rooms (from class 10000 to class 10), a chemical etching facility and an ultra-clean water supply. A UHV furnace is used to improve the niobium thermal conductivity via heat treatment at 1400 °C in the presence of Ti gettering. The last step of cavity preparation consists of a high pressure (100 bar) rinsing with ultra pure water.

The cavities are first tested in a vertical bath cryostat in superfluid helium at 2 K, the TESLA operation temperature. High peak power processing [7] as well as temperature mapping [8] and local RRR measurements through eddy currents can be applied. The 9 cell structures, once they have passed the vertical test, are welded into the helium tank. The fully assembled cavity can be tested in a horizontal cryostat in the TTF pulsed power mode (500 μs rise time, 800 μs flat-top and 10 Hz repetition rate). The performance of the main coupler, the high-order-mode (HOM) absorbers and the cold tuning mechanism is thus checked before the cavity is installed into the cryomodule.

Cavity performance can be measured either in the horizontal cryostat or after the installation into the cryomodule. In both cases the quality factor Q is obtained by measuring the RF heat load as the difference between total cryogenic losses at 2 K and the static ones. The TTF cryoplant permits precise heat load measurements at 2 K with a resolution of 50 mW (as a reference, with the TTF time structure, a cavity operated at 25 MV/m and a Q of $1 \cdot 10^{10}$ gives a heat dissipation of 0.9 W).

CAVITY FABRICATION AND PREPARATION

The cavities are fabricated from RRR 300 niobium sheets by electron beam welding (EBW). Up to now 55 cavities have been ordered to 4 European companies: a first series of 28 in 1994 and a second series of 27, with Nb-Ti flanges, in 1997.

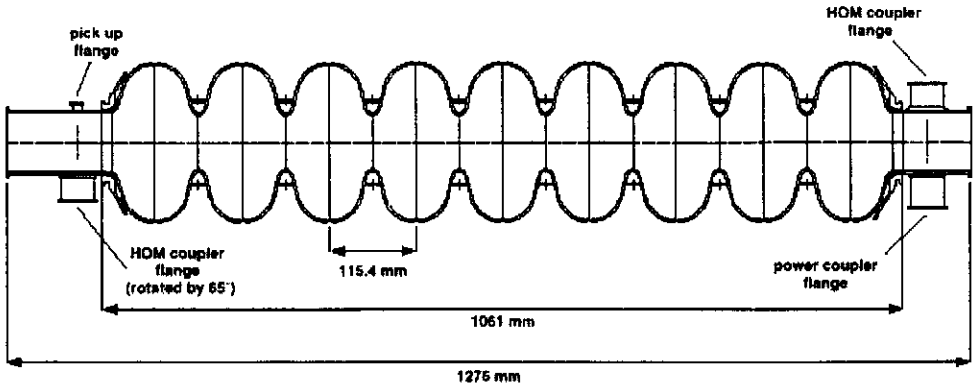

π-mode frequency f	[MHz]	1300
Active length L	[mm]	1036
Bore aperture	[mm]	70
Cell to cell coupling		1.98 %
Full cavity R/Q	[Ω]	1036
E_{peak}/E_{acc}		2.0
B_{peak}/E_{acc}	[mT/(MV/m)]	4.2
Tuning sensitivity $\Delta f/\Delta L$	[kHz/mm]	315
Loaded cavity bandwidth ($Q_{ext}=3\cdot10^6$)	[Hz]	433

Figure 2. Cross section and major design parameters of the TTF cavity. Stiffening rings are shown.

A new order for 24 cavities has being signed and the delivery is expected by January 2000. In parallel 6 special cavities (7-cell) will be fabricated to assemble a superstructure[9]. A cross section of the TTF 9-cell cavity is shown in Fig. 2, together with the main design parameters.

At present the cavity fabrication procedure includes the three following basic steps, the last two driven by the presence of the stiffening rings:

- Complete scanning of the 2.8 mm, RRR 300, Nb sheets by an eddy current apparatus [10], to discard all sheets with detected, 100 μm size, inclusions or marks.
- EB welding of the deep-drawn half cells to obtain the dumb-bells, including the stiffening ring. The iris weld is "finished" from inside.
- Completion of the cavity by equatorial EB welds performed from the outside in two subsequent passes with a fast wiggling beam. This technique[11] was found to be very powerful in making the welding parameters much less critical.

Once checked for surface status, dimensions and vacuum tightness, the cavity is delivered to DESY for acceptance tests, treatments, RF measurements and assembly. Among the large number of steps required[12] to prepare the cavity for vertical test, a partial, although significant, list is given in the following:

- Removal of 80 μm from the inner cavity surface by Buffered Chemical Polishing (BCP) and rinsing with ultrapure water, until the output resistivity is higher than 18 MΩ·cm
- Removal of 30 μm from the outer cavity surface by BCP.
- Hydrogen degassing and recrystallisation at 800 °C for two hours;

- High temperature heat treatment at 1400 °C (4 hours with Ti gettering) to improve the niobium thermal conductivity, rising the RRR from 300 to 500-700;
- 80 μm internal and 30 μm external BCP for titanium removal;
- Tuning and field profile adjustment;
- Final 20 μm BCP on the inner surface;
- High pressure (100 bar) ultrapure water rinsing (HPR);
- Drying by laminar flow in class 10 clean room, flange assembly and leak check;
- 2 additional HPR, drying as above and assembling of the input coupler.

VERTICAL TEST RESULTS

RF vertical tests include the excitation of the other 8 modes of the fundamental pass band, to determine the performance of individual cells. If required to cure field emission high power processing is applied, while T-mapping and local eddy current measurements are used to determine defect locations.

By the end of June 1999, 45 9-cell cavities have been tested in the vertical cryostat of the TESLA Test Facility. The majority of the cavities exceeded the TTF design goal of 15 MV/m and gradients up to 29 MV/m have been reached. Field values up to 35 MV/m (E_{acc}) have been achieved in individual cells by mode excitation.

Figure 3 shows the vertical test results of the 16 cavities exceeding the TESLA collider goals. Note that the cavities showing a Q_0 at low field exceeding $2 \cdot 10^{10}$ (the BCS value at 2 K) have been measured at a temperature below 2 K. All these cavities have shown a residual surface resistance of the order of 2 nΩ or less. The majority of them reached their excellent performance already in the first vertical test. Only occasionally it was necessary to repeat the last part of the preparation procedure.

The average accelerating field of all 45 cavities measured up to now exceeds 20 MV/m and that of cavities measured in the last two years is close to 25 MV/m. An overview of the time dependence of the vertical test results (the best for each cavity) is presented in Fig. 4. Since 1997, the major fabrication errors have been corrected and all the niobium sheets used for the cavity production were eddy current scanned.

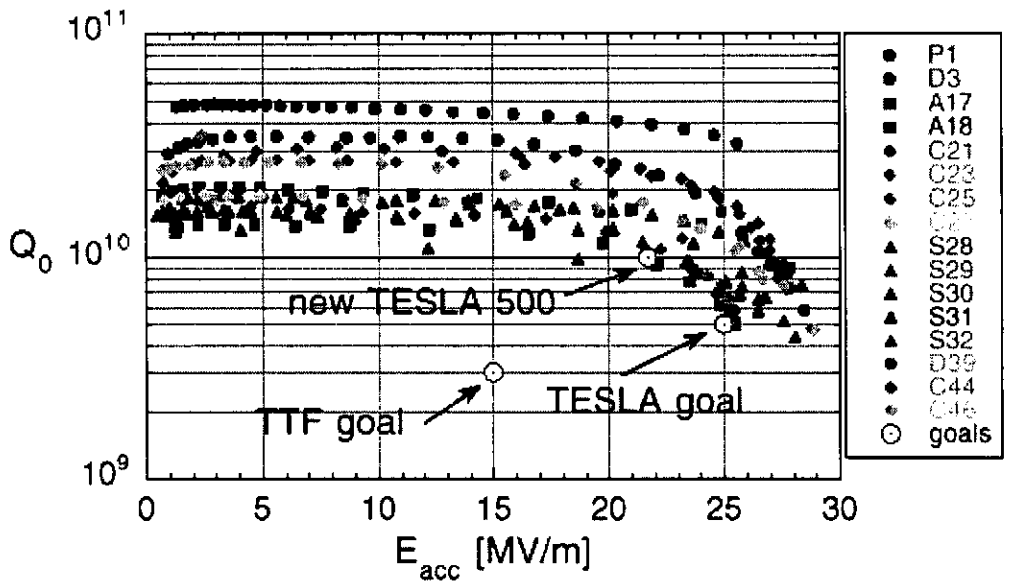

Figure 3. Vertical test results of the 16 best cavities out of the 45 measured up to now that exceed the TESLA 500 requirements. They are: E_{acc}=25 MV/m @ $Q_0=5 \cdot 10^9$ for standard 9-cell cavities and E_{acc}=21.4 MV/m @ $Q_0=1 \cdot 10^{10}$ for superstructures [9].

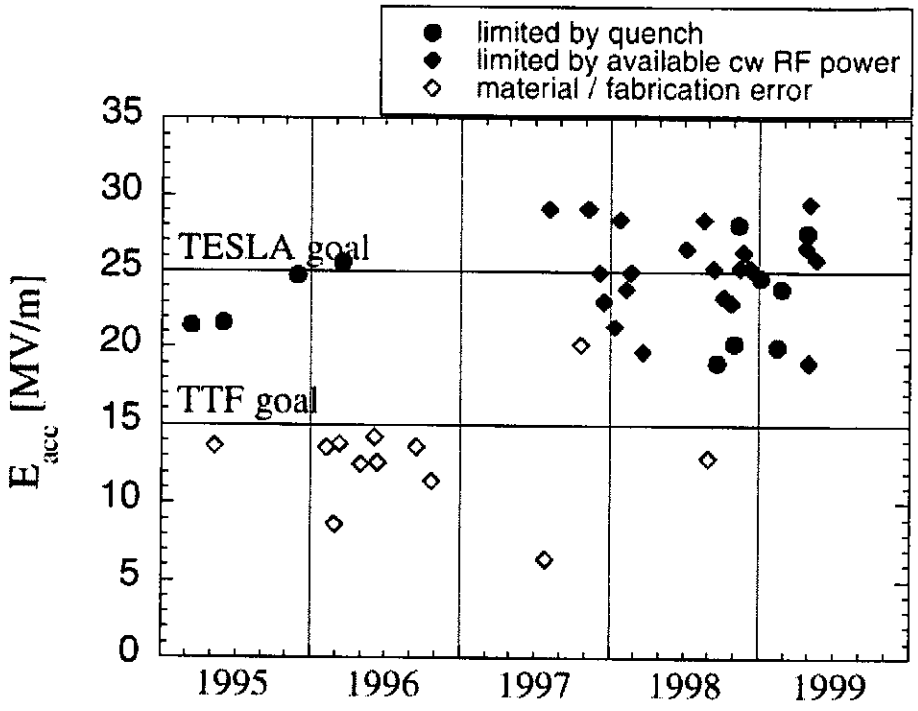

Figure 4. Overview of the time dependence of the vertical test results (the best for each cavity) for all 45 TTF 9-cell cavities measured by June 1999.

As said above, four European companies shared the production of the first two sets of cavities, for a total of 55 plus 2 prototypes. It is important to note that, once the fabrication errors were corrected, all companies have been able to produce cavities with performances exceeding the TESLA goals. At the beginning of the production the most crucial step of the fabrication procedure has been the equatorial weld[12]. Each company had to independently develop proper tooling and electron beam welding parameters. As a consequence we now have different possible procedures, all qualified for high field. In particular the final cavity assembly, by the eight equatorial welds, can be done either welding together one dumb-bell after the other, or mounting all components in a proper tool and performing the welds in a single step. Even the machining of the dumb-bell equatorial edges was based on two different philosophies and both solutions adopted, step like and flat, have proven to be adequate. At present, if no mistakes are done during the weld preparation or execution, the weld seam is no longer the region where the possible high field quenches occur. One very interesting result has been recently obtained with a cavity that had a repair performed on one of the equatorial welds. This cavity, which was supposed to be limited like the previous ones with the same defect, reached 27.9 MV/m at $Q_0=9.7\cdot10^9$. In this case the limitation was the available RF power and no quench has been detected.

HORIZONTAL TESTS AND LINAC OPERATION

After being welded into the Titanium He-tank, equipped with a motorized tuning system [13], and after the RF power coupler and the HOM couplers have been assembled, a last test prior to installation into the cryomodule is usually performed in a horizontal test stand, CHECHIA, designed and built at Saclay. The cavity performance in the horizontal cryostat in the pulsed mode is generally comparable with the results of the vertical tests [14], and with the cavity performance in the module. The small differences revealed in

some cases, in both directions, can be interpreted as due to dust particles or to the further conditioning of the field emission limit respectively.

The average gradient obtained in the 18 cavities tested so far in the horizontal cryostat is 22.5 MV/m, which does not differ substantially from the average value of 22.3 MV/m obtained in the vertical tests. One particular case is cavity C23 that reached 33 MV/m in the horizontal test with a quality factor $Q=4\cdot10^9$. In the vertical test, the cavity was limited to 25 MV/m by available RF power [15]. Most of the good cavities are at present limited by RF breakdown in the main power coupler.

The eight cavities installed in module #1 have been operated with an average gradient of 15 MV/m and the three best cavities performed close to the vertical test results [14].

The eight cavities installed in module #2 all exceeded 20 MV/m in the vertical test, but one that was limited at 19.7 MV/m by field emission. Given that no individual cavity test has been performed in the linac, it is worthwhile noting that, after proper coupler conditioning, all cavities reached 20 MV/m at full TTF pulse length and repetition rate. No further gradient increase was possible because of coupler limitations. In particular, after in-situ high peak power processing (HPP) on one cavity that was showing a very high field emission, a global RF heat load of 6.5 W was cryogenically measured at 2 K, with all cavities operating at 20 MV/m. By detuning the cavity that was still limiting the global performance, the measured RF cryogenic load given by the remaining 7 cavities was reduced to 2.9 W, which corresponds to an average Q_0 at 20 MV/m of $1.3\cdot10^{10}$, a little higher than the result from the vertical tests.

The third module has been assembled with cavities ranging from 23 to 28 MV/m, the average value being close to 25 MV/m. This module, that has been installed in place of module #1, will be cooled down and tested by the end of July 1999.

R&D ACTIVITIES AND PERSPECTIVES

The R&D activity on superconducting cavity development has grown worldwide in the recent years. This activity, that is mainly concentrated on the TESLA cavity parameters, is being done in different laboratories which are either part of the International Collaboration, or linked to it through specific Memoranda of Understanding.

Two lines can be identified according to the main tasks that are at the basis of the TESLA activity: field enhancement and/or cost reduction. In the following I just quote some promising example that can be taken as a reference. For simplicity they are divided in two subchapters: field emission and Q drop, and alternative fabrication techniques.

Field Emission and Q Drop

Since mid 1997 the average accelerating gradient of the tested TTF cavities exceeds the TESLA goal of 25 MV/m. Applying the present fabrication and processing technique developed at TTF we are now routinely obtaining cavities which exceed 20 MV/m, at $Q=10^{10}$, without field emission. Above this field level, Q starts to drop and x-ray, associated with electron emission, are usually observed. The improvement of the EB welding technique, associated with 1400 °C Ti-gettering and eddy current scanning of the niobium sheets, has raised the quench limit above the present Q drop and field emission limits.

Efforts are undertaken to further reduce field emission by improving of the HPR system and the in-situ dust particle control during assembly in the clean room. Nevertheless in the few cavities not limited by field emission the performance is limited by a different Q drop, with no electrons, of the type first observed in single cell cavities at Saclay [16]. This phenomenon has different interpretations but seems to be intrinsically related to the actual processing procedure, based on the buffered chemical polishing (BCP).

Using commercial high purity Niobium, by different suppliers, outstanding results have been obtained at KEK with a different processing technique based on electropolishing. A number of single cell cavities reached accelerating field up to 40 MV/m with a moderate Q drop starting above 30 MV/m [17]. Since this technique could have good potentiality for TESLA, both for field enhancement and cost reduction, an R&D activity in this direction on single and multi-cell cavities was started in collaboration with KEK, CERN, Saclay and industry. Recent results on multi-cell cavities at TJNL and KEK have shown that the extrapolation of the technique developed for single cell to multi-cell cavities needs further investigation. The cavity prototype P1 (Fig. 3) has been sent to KEK for electropolishing. Up to now, after two steps of moderate electropolishing, the cavity is still limited by quench at 22 MV/m. Figure 5 compares the recent KEK results with those obtained at DESY.

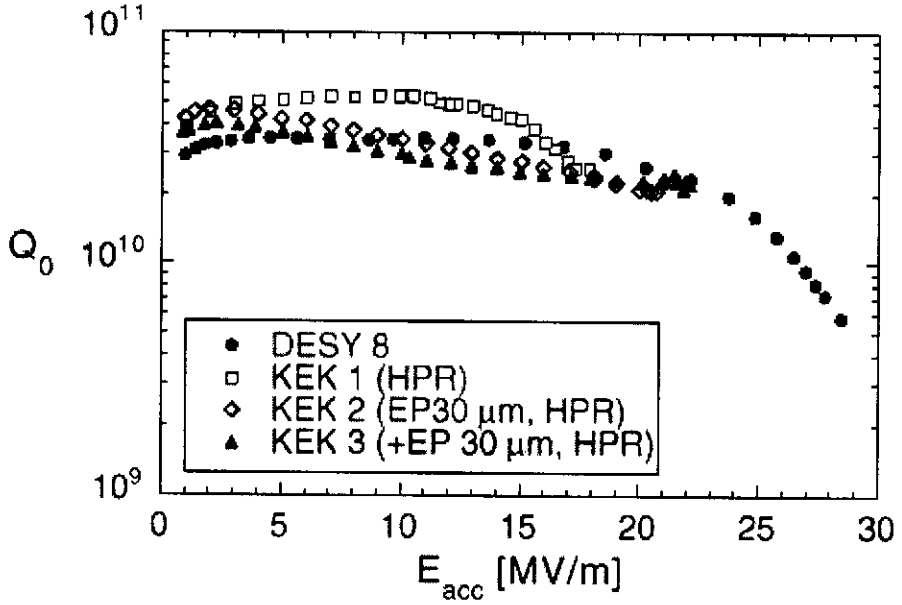

Figure 5. Preliminary results obtained at KEK with a 9 cell cavity prototype from DESY.

Alternative Fabrication Techniques

The aim of cutting cavity costs in the large scale production foreseen for TESLA drove an important R&D activity to find new cheaper techniques for cavity fabrication and stiffening. Two lines are being pursued:

- seamless Nb cavities, by spinning or hydroforming, to eliminate the equatorial welding and to slightly reduce the required niobium inventory [18];
- external thick coating of a thinner niobium cavity, to reduce the niobium inventory and mainly to perform the cavity stiffening, required to counteract the Lorenz forces in pulsed operation, at a lower cost[19].

The first line is pursued at DESY, INFN LNL, and Saclay. The results obtained so far are now approaching those of welded cavities and the application to multi-cell cavities is well advanced. At present the main limitation is still the need, for high performance, of a very deep internal surface removal (> 500 µm) to eliminate the damaged layer. A mono-cell cavity spun at LNL, while treated and measured at TJNAF, reached 33 MV/m, after a total removal of about 700 µm from the internal surface by alternating grinding and BCP [20].

The second line, proposed by IPN Orsay, using standard plasma jet spray of copper, gave initial very promising results and is now pursued in collaboration with DESY, INFN Milano and a few other partners. Different coating techniques and materials are being considered and extensive tests are under way for thermal and mechanical properties.

SUPERSTRUCTURES

Following an idea of Jacek Sekutowicz, since 1997 a growing effort is dedicated to the development and test of superstructures, which could be a challenging alternative to the present 9-cell cavities for the TESLA collider [9].

In the TESLA design [4], for a cavity accelerating gradient of 25 MV/m, the average energy gain produced by a cavity string is limited to 17.8 MeV/m because of the relatively poor cavity filling factor, 75%, defined as the percentage of the cavity active length with respect to actual cavity length. This value comes from the fact that the number of $\lambda/2$ cells per cavity is 9 and the cavity separation is $3\lambda/2$.

The proposed superstructure scheme is based on sub-units, called superstructures, made of four 7-cell standing wave cavities, coupled together through an enlarged $\lambda/2$ long beam pipe. The superstructure is fed by a single main coupler, while each 7-cell sub-structure needs an independent tuner. Five HOM couplers are envisaged for the superstructure and the risk for trapped modes is reduced. Applying the same criteria for the definition of the filling factor, with the new scheme it will grow from the present 75% to about 83%. This important saving may be spent either to increase the final energy for the same cavity gradient or to reduce the required gradient for the same energy. In addition to the increased cavity filling factor, some other advantages are expected, among then I wish to quote:

- the number of main couplers is reduced by a factor of more than 3 and the power distribution is simplified;
- the unflatness of the accelerating field, for the same geometrical errors, is reduced because it scales as the square of the number of cells (7 instead of 9).

The experimental results obtained with a warm model of the superstructure have been very encouraging and the expected RF behavior in terms of filling time, field distribution and sensitivity has been confirmed. Figure 6 shows the simplified design of the actual superstructure being ordered, to be made according to our standard fabrication and processing technique. In particular, to be compatible with the actual infrastructures at DESY, a flanged solution has been preferred, with respect to the final welded one, to connect together the four 7-cell sub-structures that constitute the superstructure prototype. We expect to start the cold RF measurements with beam, in a modified TTF cryomodule, by the end of 2000.

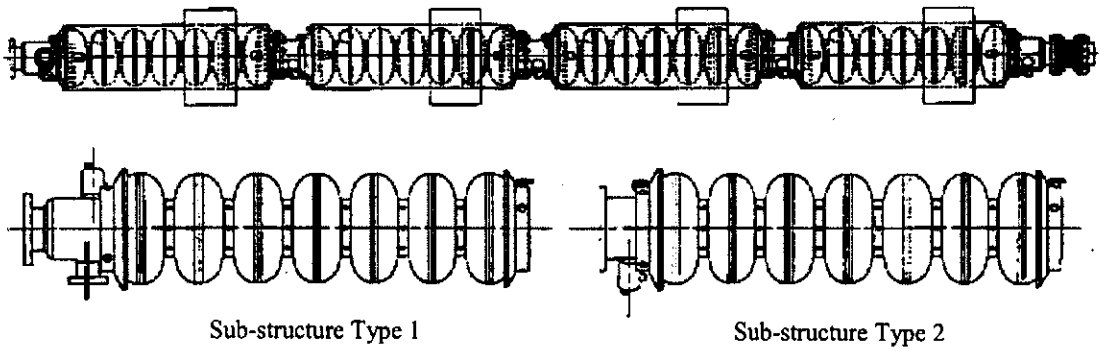

Figure 6. Simplified mechanical drawing of the niobium superstructure whose design has been completed and is being ordered in July 1999, to be cold tested by the end of 2000. An enlarged view of the two types of 7-cell sub-structures is shown in the lower part of the figure. While in the eventual final design the four 7-cell sub-structures should be welded together, we preferred the flanged solution for the prototype.

CONCLUSIONS

The results obtained so far in the framework of TTF are very encouraging and the technical possibility to build TESLA is becoming a reality. In particular the cavities are now routinely reaching the TESLA requirements and no degradation of cavity performance is found between vertical test, horizontal test and linac operation. Recent results and ideas show that even higher fields can be probably reached in the near future.

ACKNOWLEDGEMENTS

Thanks are due to all the members of the TESLA Collaboration for the excellent work done so far, and a special one to Matthias Liepe for figures and transparences.

REFERENCES

1. R. Brinkmann, Low Frequency Linear Colliders, Proc. EPAC'94, London, England.
2. H. Padamsee Ed., Proc. 1st Int. TESLA Workshop, Cornell, USA, 1990, Cornell Report, CLNS90-1029.
3. TESLA Test Facility linac - Design Report, DESY Report, TESLA 95-01, 1995.
4. Conceptual Design of a 500 GeV e+e- Linear Collider with Integrated X Ray Laser Facility, R. Brinkmann et al. Eds, DESY Report, 1997-048, 1997.
5. C. Pagani, D. Barni, M. Bonezzi, J.G. Weisend II, Further Improvements of the TESLA Test Facility (TTF) Cryostat in View of the TESLA Collider., Paper presented at this Conference.
6. S. Wolff, The Infrastructure for the TESLA Test Facility, Proc. PAC'95, Dallas, Texas.
7. C. Crawford et al., High Gradients in Linear Collider Superconducting Accelerator Cavities by High Pulsed Power to Suppress Field Emission, Part. Acc. 49, pp. 1-13, 1995.
8. Q. S. Shu et al., An Advanced Rotating T-R Mapping & its Diagnoses of the TESLA 9-cell Superconducting Cavities, Proc. PAC'95, Dallas, Texas.
9. J. Sekutowicz, et al., Superconducting Super-structures for the TESLA Collider, Proc. of EPAC'98, Stockholm, Sweden, June 1998 and DESY Report, TESLA 98-08.
10. W. Singer et al., Diagnostics of Defects in High Purity Niobium, Proc. of the 8th Workshop on RF Superconductivity, Abano Terme, Italy, Oct. 1997.
11. J. Brawley et al., Electron Beam Weld Parameter Set Development and Cavity Cost, Proc. of the 8th Workshop on RF Superconductivity, Abano Terme, Italy, Oct. 1997.
12. D. Proch, Status of Cavity Development for TESLA, Proc. of HEACC'98, Dubna, Russia, 1998.
13. Ph. Leconte et al., TESLA Test Facility Cold Tuning System, DESY Report, TESLA 93-09.
14 A. Gössel et al., Vertical and Horizontal Cavity Test Results in Comparison with Performance in the TTF Linac, Proc. of the 8th Workshop on RF Superconductivity, Abano Terme, Italy, Oct 1997.
15. C. Pagani, Developments and Achievements at the TESLA Test Facility (TTF), Proc. Applied Superconductivity Conference, Palm Desert, California, September 1998.
16. M. Pekeler, Experience with Superconducting Cavity Operation in the TESLA Test Facility, Proc. of PAC'99, New York, NY, March 1999.
17. M. Ono et al., Achievements of 40 MV/m in L-Band SC Cavity at KEK, and K. Saito, Superiority of Electropolishing over Chemical Polishing on High Gradients, Proc. of the 8th Workshop on RF Superconductivity, Abano Terme, Italy, Oct 6-10, 1997.
18. V. Palmieri, Seamless Superconducting RF Cavities, Proc. of PAC'99, New York, NY, March 1999.
19. S. Bousson et al., An Alternative Scheme for Stiffening SRF Cavities by Plasma Spraying, Proc. of PAC'99, New York, NY, March 1999.
20. P. Kneisel and V. Palmieri, Development of Seamless Niobium Cavities for Accelerator Application, Proc. of PAC'99, New York, NY, March 1999.